CHAPTER 1

Chapter 1
Introduction to the World of Hyperspectral Remote Sensing-Literature Review

SUMMARY

This chapter begins with a brief overview of remote sensing fundamentals and then moves onto the topic of hyperspectral remote sensing where the concept of spectral signatures with regards to vegetation is thoroughly discussed. The issues of hyperspectral sensors causing limitation in their widespread use are discussed in detail. Literature survey comprising of inherent issues like smile, noise, flaws in experiment design etc. is presented here. Also included is the literature survey concerning data redundancy, atmospheric correction and image classification. In context to specifications needed for future hyperspectral remote sensor for vegetation assessment, literature survey pertaining to spatial and spectral resolutions is also presented. Based on this chapter, the objectives of this work are mentioned at the end. A brief outline of all the chapters is documented, followed up by the list of references for this chapter.

1.1 INTRODUCTION TO HYPERSPECTRAL REMOTE SENSING

1.1.1 Remote Sensing fundamentals

Anything sensed from a distance is called remote sensing. Human body is a classic example of it. For example, our eyes are routinely doing remote sensing! However,

typically speaking, remote sensing (RS) refers to the science of making inferences about objects from measurements, made at a distance without coming into physical contact with the objects under study (Campbell, 2002). In this context, any force field like gravity, magnetic, electromagnetic etc. could be used for remote sensing. However, it is more common to use the term remote sensing for identifying Earth features using characteristic electromagnetic energy that is reflected/ emitted from the features on the earth. The United Nations gave a more formal definition which states, "*Remote sensing means sensing of Earth's surface from space by making use of the properties of electromagnetic wave emitted, reflected or diffracted by the sensed objects, for the purpose of improving natural resource management, land use and the protection of the environment.*" This thesis focuses on this aspect of remote sensing.

From remote sensing point of view, visible, IR and microwave portion of electromagnetic regions are most relevant, especially the Near Infra-Red (NIR) part of the spectrum because it is most suited for vegetation, as healthy green vegetation reflects more in NIR then in visible. This is why in remote sensing images green vegetation is generally shown in red colour.

As regards to source, sun is the main source of Electro-Magnetic (EM) radiation reaching the Earth. But, when solar radiation passes through the atmosphere, atmospheric gases, molecules and particulates scatter and absorb the radiation. So, the remote sensor observes energy from the atmosphere called *path radiance*, as well as from the surface (Figure 1.1).

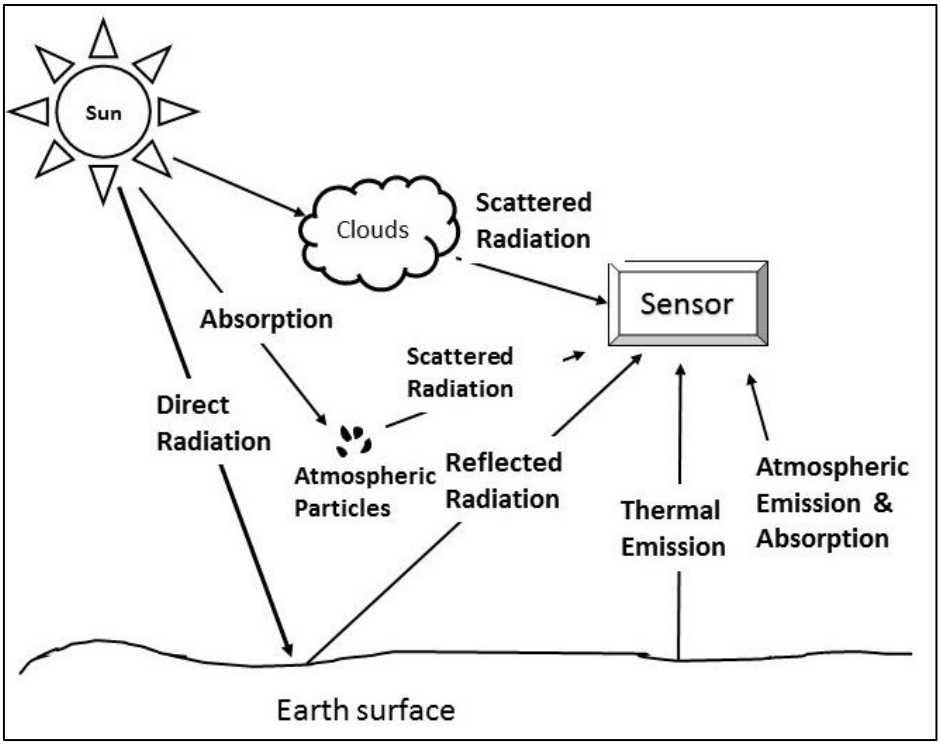

Figure 1.1: Schematic representation of radiation components reaching the remote sensor

In total, the radiance detected by the sensor includes attenuated radiance from the target on Earth and the radiance of scattered light, as shown in equation 1.

$$L=\rho e\tau/\pi+\text{path radiance} \quad (1)$$

where L=total radiance at detector, e is irradiance at Earth's surface, ρ is terrain reflectance and τ is atmospheric transmittance.

In case of atmospheric scattering, EM radiation gets scattered and redirected from its original path. The amount of scattering depends on several factors including wavelength of radiation, density of scatters etc. Independent of the mechanism of atmospheric interference, the remote sensing images are corrupt. Hence, for meaningful interpretation,

especially when quantitative interpretation is required, atmospheric influences have to be removed (Kaufman & Sendra, 1988; Liang et al., 1997; Vermote et al., 1997). This process is called *atmospheric correction*.

1.1.1.1 Types of remote sensors

Before the design of the remote sensor, care is taken in deciding upon the wavelength region of sensor operation. This is because, within the EM spectrum, there are certain regions which are heavily afflicted by the scattering and absorption by atmospheric molecules. So, remote sensors are designed in such a way so as to avoid these regions. The regions within the EM spectrum which don't have much attenuation from the atmosphere are called *atmospheric windows*. Remote sensing of Earth's surface is generally confined to these windows only. They correspond to the wavelength range 0.4-1.3, 1.5-1.8, 2.2-2.6, 3.0-3.6, 4.2-5.0, 7.0-15.0 μm and 1cm to 3 cm (Joseph, 2005). Within these atmospheric windows, two major classes of sensors are defined-those working in Optical Infra-Red region (OIR) and those working in Microwave region of the EM spectrum. The OIR region spreads from visible and NIR (commonly abbreviated as VNIR) to the short-wave infrared (SWIR) and then from 8-15μm where they are called Thermal Infra-Red (TIR) sensors. Based upon the bandwidth size, the sensors in OIR range are categorized as *broadband or multispectral* and *narrow band* or *hyperspectra*l. As is obvious from the name hyperspectral sensors have more bands with channel size smaller than broadband sensors (Barry et al., 2001). The detailed discussion on them follows in the forthcoming sections.

Sensors working in microwave region of the EM spectrum are called Microwave sensors, e.g. Synthetic Aperture Radar. Such sensors have an additional advantage of penetrating the clouds.

There is yet another way of discriminating between two classes of sensors. These are *passive and active sensors* (https://earthdata.nasa.gov). If the source of EM radiation is sun, the sensing is called passive remote sensing and sensors are *passive sensors*. On the other hand, if the source produces EM radiation of a specific wavelength/s and the sensor studies the interaction of this radiation, it is called *active remote sensing*. For e.g. RADAR and LIDAR are active remote sensing instruments.

1.1.1.2 Characteristics of a remote sensor

There are four essential characteristics of a remote sensor which define its applications and uses. These are- 1) Spatial Resolution, 2) Spectral Resolution, 3) Radiometric Resolution, and 4) Temporal Resolution

Joseph (2005) defines spatial resolution as the projection of the detector element on to the ground. So, it is important in defining the smallest object that can be imaged (Jensen, 2005; Purkis & Klemas, 2011). It depends on the Instantaneous Field of View (IFOV) and the height of the satellite orbit, which together define Ground IFOV or (GIFOV). Through its measure, pixel size on the ground is known (figure 1.2). However, it is the not the sole measure.

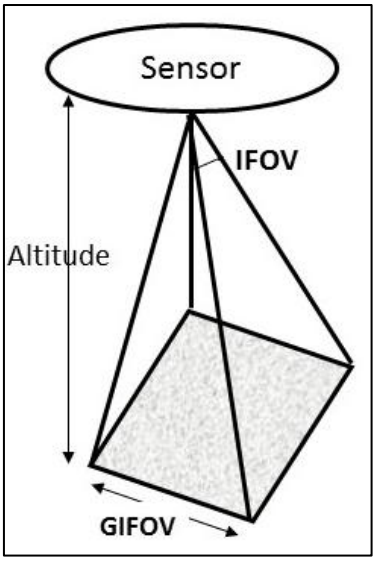

Figure 1.2: Relation between IFOV, sensor altitude and GIFOV

While defining the spectral bands of a remote sensor, central wavelength, Bandwidth and number of bands are used. The choice of central wavelength depends upon the kind of application intended. For e.g. for vegetation related studies, visible and NIR bands are generally used. The second important aspect is the spectral resolution, which is basically the spacing between the two bands (Jensen, 2005; Joseph, 2005; Purkis & Klemas, 2011). The selection of bandwidth is a trade-off between the amount of energy to be collected and spectral shape of the features to be observed. In case, the number of bands is large with small bandwidth (of the order of 10nm) or high spectral resolution and are contiguous, the sensor is called hyperspectral. In broadband sensors the bandwidth is usually of the order of 100nm and the bands are discreet.

Radiometric resolution is a measure of capability of the sensor to differentiate the smallest change in the spectral reflectance/emittance between various targets and is expressed in terms of bits (Joseph, 2005). It depends on SNR and Saturation Radiance.

For e.g., quantization of 16 bits means the radiance will be divided into 2^{16} levels. Lastly, temporal resolution refers to the time interval after which the same area is reimaged (Joseph, 2005).

Each kind of resolution has its impact on others. As a result, there is always a trade-off between the optimum set of sensor specifications (Joseph, 2005; Ose et al., 2017). *Thus, based upon the application intended, the user, must decide upon various resolutions*.

1.1.1.3 Imaging system

The remote sensors can acquire data either in the form of an image or in terms of spectral quantity or parameter as a function of time. If they create an image, they are called imaging sensors and if they don't, they are called non-imaging sensors. The sensors for atmospheric studies are often non-imaging. To capture the image, the sensors can either take a whole frame in one go (in that case they area called *framing or non-scanning sensors*) or they scan and generate the scene after the radiation from all points of the image is received via electronics for each part. If image is acquired line by line, it's called *along track scanner* and if it's acquired pixel by pixel, it is called *across track scanner*. This scanning can be from either of the two means-*whiskbroom imaging or pushbroom imaging.* In whisk-broom imaging, several lines are scanned simultaneously but in bush-broom imaging, the sensor collects a complete line simultaneously by using a linear array. The scanning techniques are shown in figure 1.3 below.

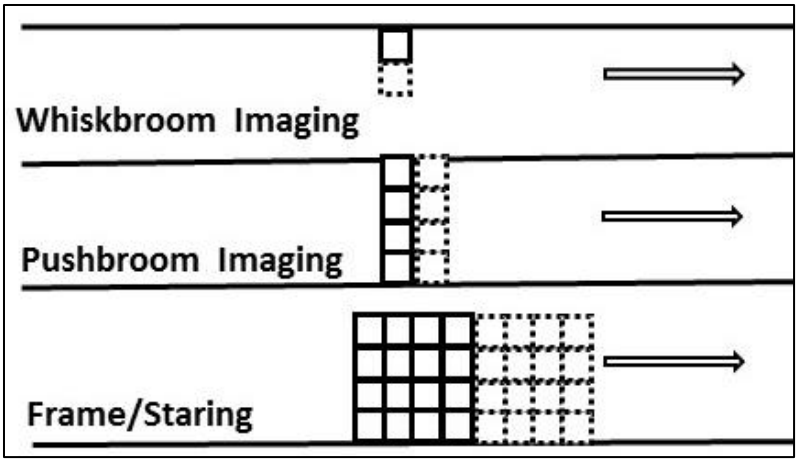

Figure 1.3: (a) Whiskbroom imaging, (b) Pushbroom imaging, (c) Framing mode

1.1.1.4 Platforms

The remote sensor needs a platform from which data capture is done. There are three basic types of platform- 1) Ground based, 2) Airborne and 3) Spaceborne (www.map.sedu.edu). The instruments used to take ground observations are usually hand-held or are positioned on a tripod or a tower. Such instruments are called ground based instruments. They are mainly used for validating the output of airborne/spaceborne studies and/or to generate spectral library. Thus, they are supposed to be accurate (www.geopool.fi). But, they cover a very small range and hence this factor must be borne in mind while conducting validation studies. Moreover, the errors due to manual handling increase in such cases. Airborne instruments are placed in aircrafts. Aircrafts can cover data from a height of 5km to 20km (https://directory.eoportal.org). So, they have better spatial resolution than spaceborne adaptations but they are time consuming and costly. At the same time, the aircraft movement causes image distortion (Homma et al., 2000), which can later be corrected. They are especially useful

for large scale topographic mapping and for damage assessment post disaster like after floods. Platforms are termed as spaceborne when they are launched in space. They orbit around the Earth and capture data at good temporal resolution. It is the most popular form of data capture due to large area coverage and due to their ability to provide better data continuity.

Depending upon the mission objective, the satellites are placed in different orbits - Low Earth Orbit (LEO) or *polar orbits,* Medium Earth Orbit (MEO) and High Earth Orbit (HEO) or *geostationary orbit*. LEO are primarily used for remote sensing purpose (Joseph, 2005).

1.1.2 Hyperspectral remote sensing

1.1.2.1 Need for hyperspectral remote sensing

Since the advent of the first remote sensing satellite, extensive studies have been done related to vegetation. Hand-held, airborne as well as satellite data (especially broadband data) were used for carrying out such observations. However, the broad band data cannot harness the information from several distinctive absorption troughs as well as reflectance characteristics including the 'red edge'. Application of broadband data is limited for species level discrimination (Anderson et al., 1976; Clark et al., 2005; Fairweather et al., 2012), for ruling out pests and disease infestation in vegetation (Ranjitha & Srinivasan, 2014), crop residue discrimination (Singh et al., 2013), weed detection (Sobhan, 2007) etc. This is because most of the broad band data have wide bandwidth (of the order of 100nm) while the diagnostic reflectance/absorption feature is confined to a few nm.

Moreover, the number of bands is also less (4-6 in general). *Within such a wide spectral region, a lot of subtle information is averaged, normalized or even hidden.* Hence, such features are not picked up by broadband data and no diagnostic study can be made. This calls for the need of remote sensing instruments based on imaging spectroscopy, called hyperspectral remote sensing instruments (Clark et al., 1995; Merton, 1999; Cochrane, 2000; Bhaskaran et al., 2001; Clark et al., 2003; Ellis, 2003; Shippert, 2004; Bannari et al., 2015; Ghamisi, 2015; Ballanti et al., 2016; Adao et al., 2017).

1.1.2.2 Hyperspectral remote sensing -Introduction

Sir Isaac Newton in 1704 gave the concept of dispersion of light, indicating that white light can be dispersed in continuous 'colours' using prisms. But, only after Fraunhofer in 1817 discovered the dark lines in solar spectrum, the quantitative measurement of dispersed light came into being. The term spectroscopy was first used in the late 19th century and provided the empirical foundations for atomic and molecular physics (Born & Wolf, 1999). Spectroscopy was first used by astronomers for planetary studies but with advances in space technology and increased awareness of the potential of spectroscopy, the first imaging spectrometers (Goetz et al., 1982; Vane et al., 1984) came into being. From remote sensing point of view, Imaging spectroscopy involves image acquisition in many contiguous spectral bands so as to produce laboratory quality reflectance spectra for each pixel in an image. Schaepman (2007) defined it as the *simultaneous acquisition of spatially coregistered images, in many narrow, spectrally contiguous bands, measured in calibrated radiance units, from a remotely operated platform.*

As the name suggests, "Hyper" means excessive. Such sensors have tens of contiguous, narrow bands. The large numbers of bands provide researchers with vast quantities of information (Goetz et al., 1985). Hyperspectral Imaging (HSI) has a spatial component and each image pixel contains spectral information over the hundreds of bands to generate a "data cube." These cubes can be mined for spectral information to use with the spatial context. HSI data are used to detect, classify, identify as well as quantify materials present in the image using diagnostic or characteristic absorption features in its spectral signature. The signature is generated by the information contained in the numerous spectral bands acquired by the sensor. The narrow bands in which radiance is measured, combined with the high number of bands allows detection of minute variations in the spectral signatures. The standard collection of these spectral signatures is called spectral library which is used to identify the material under investigation (Goetz et al., 1985).

It was in 1970s that a group of scientists (Knipling, 1970; Swain and Davis, 1978) studied the reflectance spectra of rocks, minerals and vegetation, and developed the underlying concept of hyperspectral remote sensing. From then on, airborne imaging spectrometers became available on a wider basis for Earth's studies (Kruse et al., 1990; Green et al., 1999) and for spaceborne imaging spectrometer activities (Goetz & Herring, 1989; Rast et al., 2001). However, until today there is dearth of spaceborne imaging spectrometers. The major limitation of spaceborne hyperspectral sensor is the low SNR than that on an airborne system, significantly more atmosphere influences, detector calibration issues and issues with adequate shielding of each detector so that no stray light can enter the individual detector array. Moreover, in case of designing hyperspectral sensors there always exist a tradeoff between spatial resolution, spectral resolution and

SNR. Finer spatial resolution implies that the radiation reaching the sensor corresponding to one pixel comes from smaller area and thus has less energy. The same is true for finer spectral resolution. If the spectrum is divided into a number of bands, the total energy stays equal but a single band contains less energy. It may happen that the energy due to sensor noise equals the energy of the signal. Therefore, hyperspectral sensors often have coarser spatial resolution (Landgrebe, 2003). Moreover, the choice of dispersing element, sensor responsivity etc. also makes the design of hyperspectral sensors challenging.

Imaging spectroscopy has had exponential growth over the past two decades in terms of referenced publications and associated citations (Schaepman, 2009) showing immense increase in relevance of imaging spectroscopy to Earth observations and its related research. In the field of vegetation studies, hyperspectral remote sensing has played a big role in Species composition (Christian & Krishnayya, 2009; Panigrahy et al, 2011; Manjunath et al, 2012; Singh et al, 2015), Biophysical properties (Kumar et al., 2001; Mutanga & Skidmore, 2004), Biochemical properties (Curran et al., 1990; Gitelson et al., 1996; Gitelson & Merzlyak 1997; Blackburn, 1999; Datt 1999; Gamon & Surfus, 1999; Daughtry et al. 2000; Richardson et al., 2002; Gitelson et al. 2003; Huang et al., 2005; Gao, 2006), Disease and stress (Filella et al., 1995; Moran et al., 2000; Zarco Tejada et al, 2003; Zhang et al, 2003; Muhammed, 2005), Net primary productivity (Smith et al, 2002), Crop residue studies (Daughtry et al, 2005; Bannari et al, 2006; Singh et al, 2013;) etc.

1.1.2.3 Concept of signatures

The EM radiation when incident over the surface, either gets reflected, absorbed, re-radiated or transmitted through the material depending upon the nature of the object and the wavelength of the incident radiation which, thus forms the signature of that object (Joseph, 2005). Thus, any set of observations which directly or indirectly leads to the identification of the object and/or its conditions is termed as its signature. Spectral, spatial, temporal and polarization characteristics facilitate target identification/discrimination and hence form the unique signature of the physical object. Spectral variations include changes in reflectance/emittance of objects as a function of their wavelength. Temporal variations include changes in reflectance/emittance with time (Dennison & Roberts, 2003) while polarization variation includes changes in polarization of radiation reflected/ emitted by an object. The spectral variation is the most commonly used signature (Clark, 1999; Ustin et al., 1999).

Since, this study deals with vegetation studies only and that too in reflective OIR domain; hence the physical basis of signature of vegetation in OIR region is only discussed in the following text.

When vegetation is observed from a remote hyperspectral instrument, the integrated effect of vegetation as a whole is recorded. This includes leaves, stems, branches, flowers etc. as well as the background, which in many cases is soil. Nonetheless, the major contribution is from the leaves which form the higher surface area in comparison to the other parts of the vegetation. The general shape of reflectance and transmittance curves for green leaves is similar for all species with some peaks and troughs corresponding to specific pigments and the cellular structure of the leaf tissue (Ustin et al, 1999). In the

optical part of the spectrum, the leaf's radiation regime, shape, size, internal structure, pigment concentration, water content and dry matter content (Ross, 1981) modulates the nature and amount of reflection (Liang, 2004). This leads to the characteristic reflectance curves for different vegetation species, and thus forms the fundamental for hyperspectral remote sensing of vegetation.

Structure of leaves and vegetation signature

In general, both upper and lower surfaces of the leaf are called epidermis or the skin of the leaf. It has waxy layers of variable thickness (~3-5 μm). It has large number of openings called stomata which regulate the exchange of gases and loss of water vapour from the leaves. In between the two epidermal layers lie the mesophyll tissues which consist of elongated cells arranged in rows called palisade parenchyma and/or irregularly arranged cells with large intercellular spaces called spongy parenchyma. Palisade parenchyma forms towards the light's entry point. The parenchyma cells are filled with cell sap and protoplasm. Within the protoplasm are chloroplasts which contain leaf pigments. Pigments found in general are chlorophyll, carotenes, xanthophylls etc. with highly varying distribution amongst different species (Gates et al., 1965). Chlorophyll is of two types, one is called chlorophyll-a ($C_{55}H_{72}MgN_4O_5$) and the other is called chlorophyll-b ($C_{55}H_{70}MgN_4O_6$). Chlorophyll-a is found in all photosynthetic plants. These pigments have distinct absorption regions, which forms the main strength of hyperspectral remote sensing. Besides the leaf pigments, the leaf constituents that take part in the interaction are cell wall, chloroplasts, cell sap and air.

Plants absorb radiation throughout the UV and visible regions of the EM spectrum for photosynthesis. In NIR region, plants have poor absorption and then good absorption again at 2.5 μm. When sunlight is incident over the leaf surface, majority of it is reflected specularly (Woolley, 1971). The amount and nature of reflected light varies with species because the leaf surfaces (cuticles) have different amount of wax layers on it. Rest of the energy reaches the internal structure of the leaf and interacts with them either through reflection, refraction, scattering or transmission. Different sun-rays, on entering the leaf, encounter different geometries; as a result, they are reflected/ transmitted/refracted/scattered in different directions. Some light gets absorbed as well. Reflection/refraction occurs on account of various kinds of interfaces/discontinuities like cell sap-cell wall, cell wall-air etc. which lead to changed index of refraction. The radiation observed for the canopy cover by a remote sensor consists of the integrated effects of leaf layers, branches, twigs, fruits, flowers and adjacent ground areas as well as the shadow. When vegetation cover is sparse, the effect due to background dominates and contaminates the spectra from pure vegetation. The arrangement of vegetation, sun and view directions also play a considerable role. For example, when plants are planted in rows and sun rays fall all along the rows, the bare soil is fully illuminated while when the sun rays fall across the rows, the soil comes in the shadow region of the standing vegetation. Thus, in both the cases the observed spectra will be different (Joseph, 2005).

Typical spectra of a leaf

The spectra of the leaf spreads along visible through SWIR region. In the visible region, the major role in the spectra is played by leaf pigments through the process of absorption

by chlorophyll, peaking at around 550nm. The reflectance in this region is low (~10%). The spectra observed NIR range of EM spectrum mainly arise from the internal structure of the leaf (Woolley, 1971; Gausman, 1974; Slaton, 2001). Around 40-50% of energy is reflected within this range while <5% is absorbed. The reflection is mainly owed to the multiple reflections within the mesophyll structure as well as its arrangement. Since, internal structure changes with the species, the vegetation spectrum is largely distinct in this range of wavelengths. The SWIR region is characterized by water content of the leaf (Seelig et al., 2008; Mobasheri and Fatemi, 2013). Hence, this region has three strong water absorption channels (1400nm, 1900nm, 2700nm). So, any water deficit within the plant species will show in this wavelength region. Therefore, with decreasing moisture content of the leaf, the reflection in this region increases. Figure 1.4 shows the characteristic vegetation spectra from visible through SWIR region while explaining the important absorption regions.

Reflectance from Vegetation Canopy

The radiation observed for the whole canopy consists of the integrated effects of leaf layers. This radiation is called canopy reflectance instead of leaf reflectance. The stack of leaf changes the amplitude of various values though the pattern of the spectrum remains unchanged (Neuwirthova et al., 2017). Factors corresponding to the plant physiology lead to identification and discrimination of various types of vegetation. For e.g. during plant senescence, because of chlorophyll reduction, high reflectance is observed in the visible region (Knipling, 1970). Gausman et al. (1971) have demonstrated the difference in reflectance spectra among 11 plant genera due to internal structure and water content.

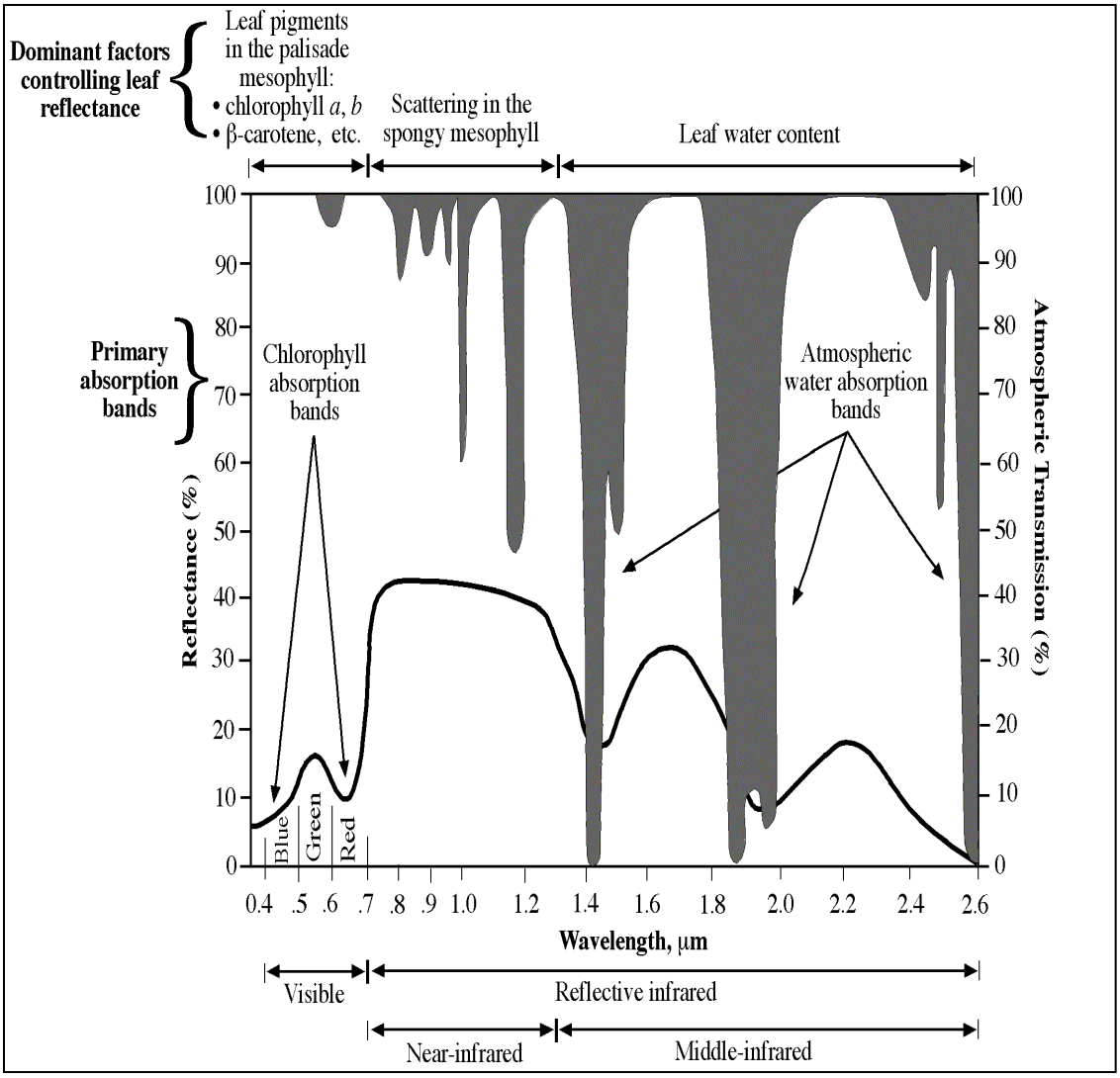

Figure 1.4: Spectrum of green leaf (Source: Hoffer, 1969)

1.1.3 Hyperspectral sensors

In 1972, after the launch of Landsat-1, NASA initiated a study to evaluate Landsat-1's capability for geologic mapping. After this unsuccessful step, first Portable Field Reflectance Spectrometer (PFRS) working within the range 0.4-2.5μm of the solar spectrum was developed in 1974 (www. photoncs.com). The outcome of its study led to

the development of band 7 of Thematic Mapper and later helped in the development of Airborne Imaging Spectrometer (AIS). The development of terrestrial imaging spectroscopy started in the late seventies by NASA's Jet Propulsion Laboratory (JPL) and a government of Canada/private partnership (Department of Fisheries and Ocean/Moniteq) leading to the Airborne Imaging Spectrometer (AIS; Vane & Goetz, 1988) in the U.S.A. and the Fluorescence Line Imager (FLI; Hollinger et al., 1987) in Canada with first data acquisitions in 1983 and 1984, respectively. With these efforts, JPL's Airborne Visible/Infrared Imaging Spectrometer (AVIRIS) came into being (Vane et al., 1993) and in 1988 Compact Airborne Spectrographic Imager (CASI; Anger et al., 1990) was developed. Many more airborne systems have been developed since that time (Buckingham, 2008).

The first space-borne hyperspectral system successfully launched was NASA's Hyperion on EO-1 that went in orbit during 2000 (Pearlman, 2003). Compact High Resolution Imaging Spectrometer (CHRIS) on board ESA's Project for On-Board Autonomy (PROBA) platform was launched in 2001 (Barnsley et al., 2004). Both systems provided imagery in VNIR (CHRIS) and VNIR/SWIR (Hyperion). India joined the space-borne hyperspectral group with Hyper-Spectral Imager (HySI) on board the Indian Microsatellite 1 (IMS-1), working in VNIR range. China launched its hyperspectral satellite HJ-1A in 2008. In 2009, a year later, NASA's Hyperspectral Imager for the Coastal Ocean (HICO) started operating from the International Space Station (Corson et al, 2008). Except HICO and HJ-1A, all others were developed for technology demonstration.

With the launch of hyperspectral missions, many advances in the data handling, atmospheric correction procedures and spectral linear unmixing, were developed (Staenz & Williams, 1997; Neville et al., 2008). These advancements also lead to the release of the first commercial Image Processing system, ENVI, in 1994 (Boardman et al., 2006). Hyperspectral image analysis modules also came up with the ongoing image processing software like ERDS Imagine and PCI Geomatica.

Table 1.1 summarizes the major spatial and spectral characteristics of the spaceborne hyperspectral sensors including the planned ones. It may be noted here that all of these sensors cover the VNIR portion of the electromagnetic spectrum with the exception of Hyperion, which in addition, acquires data in SWIR region. The ground sampling distance (GSD) varies from 17 m (CHRIS) to 500 m (HySI) and swath width from 7.65 km (Hyperion) to 129.5 km (HySI). The spectral resolution of these sensors is $\leq$ 10 nm with the exception of CHRIS whose bands vary from 5.6 nm to 32.9 nm. The latter is capable of acquiring image data from the same area on the ground under five different viewing angles (-55°, -36°, 0°, 36°, 55°). HICO had a unique orbit (space station), which restricts imaging areas up to mid-latitudes (e.g., up to 53° north). Unfortunately, HICO and Hyperion, both are not operational any more. In GISAT, Thermal Infrared (TIR) bands are also included which provides with a 500-km swath width (1500 km for the TIR sensor).

Table 1.1: Spectral and spatial characteristics of missions currently in operation, under construction and in planning stage

Sensor	Organization	Ground Sample Distance (GSD) in metre	Swath at nadir	Wavelength coverage (nm)	No. of bands	Spectral resolution (nm)
Hyperion	NASA	30	7.65	357-2576	242	10
CHRIS	ESA	17/34	13	400-1050	6/18/37	5.6-32.9
HJ-1A	CAST	100	50	450-950	110-128	5
HySI	ISRO	506	129.5	400-950	64	10
HICO	NASA	90	42	353-1081	128	5.7
GISAT	ISRO	320 (VNIR) 200 (SWIR)	160 (VNIR) 190 (SWIR)	375-2500	158 (VNIR) 256 (SWIR)	5 (VNIR) 10 (SWIR)
PRISM A	ASI	30	30	400-2500	237	12
HISUI	METI	30	15	400-2500	185	10 (VNIR) 12.5 (SWIR)
EnMAP	DLR	30	30	420-2450	218	5/10 (VNIR)10 (SWIR)
FLORIS/FLEX	ESA	300	100-150	500-780		0.3-3
HYPXIM	CNES	8	16	400-2500	>200	<10
HysPIRI	NASA	6	145	380-2500	>200	10
SHALOM	ISA/ASI	10	10	400-2500	200	10

Many countries have their own airborne sensors, for e.g., NASA has AVIRIS and India has AIMS. Airborne hyperspectral sensors combine high spectral resolution with high spatial resolution and are not so affected by atmospheric perturbation (Steinberg et al., 2016). Thus, they have played a key role in the development of hyperspectral science and applications (Kruse et al., 2003; Guanter et al., 2016), especially, Compact Airborne Spectrographic Imager (CASI), Airborne Visible/InfraRed Imaging Spectrometer (AVIRIS), Digital Airborne Imaging Spectrometer (DAIS), Reflective Optics System Imaging Spectrometer (ROSIS), Airborne Imaging Spectrometer for Applications (AISA), Hyperspectral Digital Imagery Collection Experiment (HYDICE), Multispectral Infrared Visible Imaging Spectrometer (MIVIS), etc. However, airborne sensors, have a very restricted spatial coverage, unsystematic data acquisition routines and high costs of operation. Nonetheless, they are important to serve for the specific needs and more importantly to lay foundations for the spaceborne missions.

India has two airborne missions which are flown as per the requirements. These are Airborne Imaging Spectrometer (AIMS) and Airborne Hyperspectral Imager (AHySI) working in wavelength regions 375-1000nm.

1.2 ISSUES WITH HYPERSPECTRAL DATA

1.2.1 Inherent issues

Hyperspectral data, especially the airborne and spaceborne sensors have quality issues mainly due to sensor artefacts and erroneous calibration leading to issues such as smile/frown, keystone, low Signal to Noise Ratio (SNR) etc. Moreover, the type of

sensing technique used places severe demands upon image processing systems, analysis algorithms, image cube visual display and data storage systems. These issues need to be addressed beforehand so as to maximize their full potential (Staenz, 2002; Khurshid et al., 2006). The details of these issues are discussed in the forthcoming text.

Smile and Keystone

Hyperspectral sensors have two kinds of imaging mechanisms, pushbroom and whiskbroom. When a sensor is built with linear detector arrays, it is referred to as a whiskbroom sensor. In this kind of sensor, the spectrum of each pixel on the ground is dispersed across the linear array. Airborne Visible/Infrared Imaging Spectrometer (AVIRIS) is an example of a whiskbroom sensor (https://aviris.jpl.nasa.gov). When the sensor is built with area array detectors, it is referred as a pushbroom sensor. In such a sensor, one dimension of an array is used for spatial imaging, and the other for spectral imaging. The Hyperion sensor onboard NASA's EO-1 satellite platform (Ungar, 2003) is an example of a pushbroom sensor. Pushbroom imaging spectroscopy systems often experience vertical stripping, spectral curvature effect, or smile/frown, owing to system optics (Jupp et al, 2003) and keystone interferences (Davis et al, 1999). Due to the intrinsic light dispersion properties of grating spectrometers and to minor misalignment of optical components or due to aberrations in the collimator and imaging optics, the wavelengths for pixels near the center of an array and those near the edges of the same array can be slightly different because spectral response becomes non-uniform for the cross-track dimension. This is often referred as the ''smile'' or ''frown'' effect (Mourioulis et al., 2000; Jupp et al, 2002; Neville et al, 2003). The degradation of

sensor's spectral calibration (Jacobsen et al, 2000) often leads to this. The band central wavelengths also shift due to spacecraft/aircraft vibrations or due to changes in instrument temperature and pressure (Gao et al., 2004). Smile effect is significant and observed in the spectral domain (Biggar et al, 2003) as shift in wavelength from their ostensible band positions. Consequently, the coherent analysis of the spectra making the image turns into an erratic task (Ceamanos et al, 2010). Also, it affects the proper retrieval of surface reflectance (Staenz et al, 2002) particularly in the spectral regions affected by sharp gaseous absorption features, which demand high radiometric and spectral accuracy of hyperspectral data (Green, 1999) for effective atmospheric correction. The atmospheric gas absorption features are very sharp and errors in wavelength calibrations can produce significant errors in the retrieval of land or ocean surface reflectance around these features. Atmospheric correction algorithms are typically applied to imaging spectrometer data to remove the effects of atmospheric gas absorption, and Rayleigh and aerosol scattering (Gao et al., 1993). Due to smile effect, the resulting atmospheric correction may be insufficient, leading to a noisy reflectance product; consequently, the spectra-based results like classification may be erroneous (Dadon et al, 2010a).

On the other hand, keystone effect is caused by spatial mis-registration which corresponds to band-to-band mis-registration (Davis et al., 1999). It is, however, difficult to account for and correct. Nonetheless, both smile and keystone distort the spectral features and thus reduce classification accuracy.

Thus, smile detection is necessary. Many people use Minimum Noise Fraction (MNF) as smile indicator but it has its own limitations (Dadon et al., 2010a; Jupp et al., 2002). The

smile effect appears in the first MNF component as a brightness gradient (Goodenough et al, 2003). Other methods include Trend Line Correction method (Dadon et al., 2010b); correlating sensor measured spectra with model spectra (Liao et al., 2000; Pearlman et al., 2003; Neville et al., 2003; Neville et al., 2008); phase correlation method (Yokoya et al., 2010), band difference images around atmospheric absorption features (Jupp et al., 2002) correction through column mean corrections (as in global destriping), applying a polynomial correction to the gray scale gradient in MNF-1 etc. In fact, Yokoya et al (2010) showed that smile property can be detected when a spectral signature in the correlation window contains a clear atmospheric absorption line. They also showed that by estimating spectroscopic image distortions in spectral and spatial directions, smile and keystone properties can be detected. Neville et al (2003) described the method for smile correction as the one that uses the atmospheric absorption features combined with selected Fraunhofer lines in the exo-atmospheric irradiance as spectral calibration references. Many studies have shown use of cubic spline interpolation for smile and keystone correction because of its good trade-off between smoothness and shape preservation (Feng & Xiang, 2002).

Dadon et al (2010a) summarized that any smile correction methodology must consist of at least three stages: smile detection and quantification; correction of the detected cross-track variation; and evaluation of the correction performance in light of the user requirements. For registration per se, it should be in the range 0.1 to 0.2 pixels (Engel & Weinstein, 1983, Running et al., 1994). Higher level should be addressed in the level 1 processing to obtain the at-sensor radiance (Schla¨pfer et al., 1998). *At this point, it is*

important to know the several dimensions of smile and its presence in the image. It is also important to know its influence on vegetation assessment.

Noise/Striping

One of the most important problems of using hyperspectral data is signal noise levels. Normally, noise level in hyperspectral data is high because narrow bandwidth can only capture very little energy, which, at times, is less than the system noise itself. Additionally, physical disturbances like changes in light illumination and atmospheric states make the situation worse (Landgrebe, 1997; Lyon, 2004). The system noise may be produced by numerous factors including thermal effects, sensor saturation, quantization and transmission errors which degrades the interpretability of the data (Corner et al, 2003). Radiometric noise is one of the major causes of degradation which is mainly an outcome of by photonic effects in the photon detection process, by electronic devices, and by quantization (Christophe et al, 2005). Noise due to system optics includes image smoothing along the spatial and spectral dimensions (Liao et al, 2000).

Striping is the most common form of artifact that is observed in the hyperspectral images. Many of the hyperspectral images suffer from moderate to severe streaking, may be due to differences in response across the detector array. This implies that one column may have different quantum efficiency than the successive column leading to difference in brightness between the neighbouring lines. The streaks (mainly wavelength dependent) may hamper the correct information retrieval from the data. Therefore, image destreaking is required to 'clean up' the image. Several destriping methods have been proposed in the

past (Tsai & Chen, 2008; Sun et al, 2008). However, such methods are complicated and difficult to replicate accurately.

No doubt, estimation and correction/removal of noise contained within a hyperspectral image (noise is independent of the data) is thus essential to eliminate the effects of noise contamination.

The quality of digital remote sensing data is directly related to the level of system noise relative to signal strength, expressed as Signal-to-Noise Ratio (SNR). Though the noise levels for a given sensor are generally fixed, for remote sensing data acquisition, the signal portion of the SNR is affected by other external factors such as solar zenith angle, atmospheric attenuation and scattering, and surface reflectance, which modify the signal available to the sensor (Colwell, 1983). One common means for determining an approximate SNR for remote sensing data is to use a mean/standard deviation method (Green et al, 1999; Pearlman et al, 1999). This approach requires a spectrally homogeneous area, for which mean and standard deviation are computed. SNR are normalized to 50% reflectance for comparison. This SNR is termed as "Environmental SNR," and should be considered as a lower limit on performance (Kruse et al, 2003).

Han and Goodenough (2008) emphasized that noise reduction in hyperspectral imagery is usually conducted through feature reduction in terms of data transformation, including, among others, Principal Component Analysis (PCA) (Eklundh & Singh, 1993), Maximum Noise Fraction (MNF) (Green et al, 1988), and Wavelet Transform (Bruce & Li, 2001). In all of these methods, hyperspectral data are assumed to be realizations of linear stochastic processes that are free of nonlinearity and dynamical variations. However, according to Karekes & Landgrebe (1991), physical processes like solar

radiation, atmospheric scattering, interactions between solar radiation and the Earth's surface, and responsivity of the sensing instrument etc., involved in generation of hyperspectral images, contradict this assumption. These processes may introduce nonlinearity to hyperspectral data. Bachmann et al (2005) observed this nonlinearity in hyperspectral imagery. Vaiphasa (2006) briefed that spectral smoothing and aggregating techniques including both linear and non-linear methods are popularly used in a large number of modern hyperspectral remote sensing studies for removing noise from the spectral data (Vaughan et al., 2003; Smith et al., 2004; Thenkabail et al., 2004; Wu et al., 2005). Smoothing methods, however, cause changes to the original spectral data that could lead to incorrect results in subsequent analyses (Savitzky & Golay, 1964; Tsai & Philpot, 1998; Schmidt & Skidmore, 2004). For example, plant biophysical studies (Bruce & Li, 2001; Zarco-Tejada et al., 2001; Meroni et al., 2004) and vegetation discrimination and classification (Tsai & Philpot, 2002; Foody et al., 2004; Schmidt et al., 2004) are dependent upon statistical estimates of spectral data that are often dampened by smoothing filters. Therefore, such techniques are required, which remove noise not at the expense of data corruption. Hyperspectral image analysis can be improved by effective noise estimation and removal as was demonstrated by Carmona et al (2013) and Nicholson et al (2013). *Nevertheless, noise estimation in hyperspectral images remains a challenging problem since noise may be both spatially and spectrally correlated.*

Range of values

The satellite instruments are well calibrated and validated prior to launch. However, with time dependent wear and tear, owing to thermal, mechanical, electrical and UV effects, the response of the instruments changes. Thus, there is a need to check for the data range from time to time. Second issue that interferes with the data interpretability is the sun angle and view angle change which change the understanding of the data because in different settings, the range of radiance varies for the same target (Ranson et al., 1985; Royer et al., 1985; Lord et al., 1988; Goodin et al., 2004; Schiefer et al., 2008).

Experimental Errors

While data acquisition through any of the remote sensing modes, certain issues exist, which, if not taken care of, introduce severe errors in end results. Some of them are discussed in the subsequent sections.

Change in exposure time

Exposure time refers to the duration for which a target is exposed to the camera for image capture. The number of line images that can be captured in one second, depends on the settings of exposure time, apart from others. Generally, the shorter the exposure time, the higher is the frame rate (Yang et al., 2003). With greater exposure settings, it is possible to obtain greater range of DN values i.e. the radiometric range increases, thereby, increasing the interpretation capacity of such an image (Orych et al., 2014). But, this may cause image to blur (Lelegard et al., 2010). Thus, there is a trade-off between the right exposure time so as to avoid motion blur and get images of high brightness values.

Leaf stacking

While measuring leaf's optical properties, observations can be made to single leaves (Eitel et al., 2006) or in a stack of several leaves (Gao, 1996). In case of leaf overlapping, additional variability in leaf spectra arises due to higher LAI (leaf area index) (Blackburn, 1999). Furthermore, mode of scattering at the interface of individual leaves in a stack also influences the resulting sample reflectance (Neuwirthova et al., 2017). Quantification of impact of leaf stacking on reflectance is necessary when magnitude of the spectra is considered in any study.

Phenological variations

Many important ecological processes vary with leaf age. They exhibit variable photosynthetic rates (Field, 1983; Pantin et al., 2012), morphological changes (Maksymowych, 1973), pigment change (Wilson et al., 2001; Pantin et al., 2012) and defence mechanism (Coley & Barone, 1996; Wang et al., 2012). In the vegetation spectra, the visible range of reflectance comprises of three major vegetation pigments that absorb strongly in the visible spectrum leading to unique spectral signatures and signature colour of the plant (Curran, 1989). Carotenoid pigments that absorb in the blue-green spectral region are responsible for absorbing incident radiation and for providing energy to photosynthesis (Young et al., 1990; Bartley et al., 1995). Anthocyanins absorb strongly in the green and red region provide photoprotection as well as physical damage protection (Chalker-Scott, 1999; Steyn et al., 2002). Both carotenoids and anthocyanins have overlapping absorption regions with chlorophyll absorption. With phenological changes, the pigment concentration and leaf's shape, size and surface changes leading to

variation in their reflectance characteristics (Beamish et al., 2017). Thus, without the knowledge of the phenological stage of the vegetation, the user may commit serious errors in interpretation. *To what extent the damage in assessment may occur needs to be known.*

Species consideration

Several researchers have been able to estimate species diversity using remotely sensed data (Asner et al., 2012; Feret & Asner, 2014). The diversity in species is estimated by examining variability in spectral features (Asner & Martin, 2008; Rocchini et al., 2010), including those associated with pigments. Hyperspectral remote sensing can be used to detect pigments quickly and non-destructively as reported by many researchers (Asner et al., 2007; Gamon & Berry, 2012). Ustin (2011) has shown invasive species identification from native species based on hyperspectral signature. Klančnik and Gaberščik (2016), too, showed spectral variations within species. Cochrane (2010) used hyperspectral data for species level classification of tropical forests. Thus, consideration of species is important while inferring from the available spectrum.

Others

Factors like saturation radiance and quantization play a great role in deciding upon the calculation of radiance values from DN (Bhatnagar et al., 2009). Thus, consideration of these is important while comparing/validating the two datasets. Accurate spectral reflectance measurements from the field are needed for vicarious calibration of satellite sensors (Slater et al., 1987), atmospheric correction (Moran et al., 2001), and to develop

and test surface reflectance models (Kimes & Deering, 1992). Field Spectroradiometers are generally used for this purpose (Milton, 1987, 2009). In all of these cases, the observation should be accurate (Pfitzner et al., 2011). Although there is no control over the inherent errors with the instrument design like Lambertain cosine response error (Myers, 1997), but the errors due to experimental conditions which greatly affect the outcome can be managed with little care. The experimental errors include uncertainties in measured solar irradiance (Peterson et al., 2017), illumination and view angles and field of view (Hueni et al., 2016), adopting a robust sampling strategy, presence of stray light, improper white reference calibration (ASD, 1999; Pfitzner et al., 2011), the proximity of adjacent objects (Kimes et al., 1983) etc. Most of the time, the sky conditions are much more variable and the level of uncertainty is much higher. For example, an uncertainty of 5–10% in clear-sky irradiance has been reported by Duggin & Philipson (1982) which has led to such observations which don't match up well with the hyperspectral sensors onboard thereby lead to diagnostic errors.

The Spectroradiometer must fulfill three criteria: traceability, repeatability and reproducibility (Fox, 2001). Traceability refers to comparisons with recognized international standard. It required stable reference panel and linearity of the Spectroradiometer. Traceability is more difficult to achieve if it is necessary to measure radiance in the field, as opposed to reflectance, especially if the instrument is affected by temperature changes (Duggin & Philipson, 1982). Repeatability refers to the closeness of the agreement between the results of successive measurements of the same target carried out under the same conditions. It is a property of the Spectroradiometer. Modern field

Spectroradiometers generally have high levels of repeatability. Nevertheless, cross verification of the observations need to be made.

1.2.2 Data redundancy

Due to large number of very narrow spectral channels, Hyperspectral data has many spectrally correlated bands. This means a large number of bands have redundant data which curtail the profitable use of the data (Zhang et al, 2006). It calls for the reduction in the number of features without a significant loss of information and is called dimensionality reduction (Fukunaga, 1990; Li et al, 2013; Tan et al., 2014). It may improve the accuracy during the classification process (Plaza et al., 2009). This is because, in traditional supervised classification, the Hughes phenomenon (Hughes, 1968) exists thereby causing classification accuracy to decrease (Jimenez & Landgrebe, 1998). To overcome the Hughes phenomenon, a pattern recognition approach can be taken where the original hyperspectral bands are considered as features, and "feature-reduction" algorithms are applied (Shaw & Manolakis, 2002).

Dimensionality reduction can be achieved in essentially two ways: feature extraction and feature selection (Webb, 2002). Feature extraction involves finding the transformation from a higher dimension to a lower dimensional feature space with most of the desired information content preserved (Lee & Landgrebe, 1993). Examples of such techniques are principal component analysis (Webb, 2002; Wang et al., 2006), discriminant analysis (Fukunaga, 1990; Du & Chang, 2001); minimum noise fraction transform (Philips et al., 2008), wavelet transform (Salehia & Valadanzoe), non-parametric weighted feature extraction (Yang et al., 2010) and spectral mixture analysis (Chang et al., 2002). Since, in

feature extraction techniques, a new feature space is generated, hence, the physical meaning of the original data is changed (Li et al., 2013). Feature selection, on the other hand, is used to identify the variables that do not contribute to the classification process. Such variables are removed from analysis (Webb, 2002). In short, a subset of the original bands is created. As compared to feature extraction, feature selection is a simpler and direct approach, however, extraction methods can be expected to be more effective (Serpico & Moser, 2007). The choice of technique depends upon the problem at hand (Lodha & Kamlapur, 2014) and this dimension needs to explored for different kinds of vegetation assessment.

1.2.3 Image classification

Hyperspectral data classification is a challenging task due to the presence of a large number of bands since the data dimension is huge for conventional classifiers (Luo & Chanussot, 2009). Traditional classification methods such as supervised Maximum Likelihood classification are dependent on good training classes which involves significant number of pixels to describe the spectral signature of each class and that the spectral classes must be well separated. Swain & Davis (1978) recommend 10 to 100 pixels per class per feature for proper statistics to be performed. Owing to a very large number of bands in hyperspectral data, such a kind of training would involve computationally huge number of pixels. So, alternative methods for classification are necessary like spectral matching. In this method, mapping is based on the comparison/matching of individual image spectra to a spectral library. Binary encoding

followed by spectral matching is a simple method that is sensitive to band positions but insensitive to albedo variations (Kruse et al., 1993). It encodes the data and reference spectra into 0s and 1s dependent on whether bands lie below or above the spectrum mean. Spectral angle mapper (SAM) matches image spectra to reference spectra in n-dimensions by comparing the angle between a reference spectrum considered as an n-dimensional vector and each pixel vector in n-dimensional space (Kruse et al., 1993). The spectral angle distance is independent of the magnitude of the spectral vectors and therefore insensitive to illumination and view angel variations (Kruse et al., 1993). Spectral mixture analysis is based on the general concept that pixels are not pure but are a mixture of the ground target reflectance within a single pixel. The pure targets that make up the spectral mixture of a given image are called the image endmembers. In unmixing, linear unmixing of all spectral endmembers in an image is done (Kruse et al., 1993; Gamon et al., 1999). Other methods include K Nearest Neighbour method and Support Vector Machines (SVM) (Marconcini et al., 2009) etc.

Like dimensionality reduction technique, choice of a suitable hyperspectral-centric classifier is necessary in order to improve upon the classification accuracy.

1.2.4 Atmospheric correction

The energy reaching the sensor consists of absorption and scattering by the atmosphere and the surface. Scattering and absorption by air molecules attenuate the transmission of solar radiation through the atmosphere (Iqbal, 1983). On an average, 10 percent of the radiation measured at a satellite at 1000nm is made up of scattered light (Gao et al.,

1993). Atmospheric correction is, thus, an essential preprocessing step to remove the atmospheric and solar illumination influence on the recorded signal and to derive the spectral reflectance signature of the ground surface (Staenz 1992; Richter, 1996). The main molecular absorbers in the atmosphere being water vapor (H_2O), carbon dioxide (CO_2), ozone (O_3), nitrous oxide (N_2O), carbon monoxide (CO), oxygen (O_2), methane (CH_4), and nitrogen (N_2). Major atmospheric water vapor absorption bands are centered at ~ 940, 1140, 1380 and 1880 nm, a strong oxygen absorption band at 762 nm, and a carbon dioxide absorption band near 2080 nm.

Atmospheric correction can be done through relative as well as absolute methods. While the methods like empirical line approach, internal average relative reflectance, flat field approach (Kruse, 1988) fall under relative correction techniques, use of a radiative transfer (RT) code is absolute. The Internal Average Reflectance (IAR) approach calculates the average spectrum of a scene. The spectrum of each pixel is then divided by the average spectrum to estimate the relative reflectance spectrum for the pixel. This approach is mainly applicable for vegetation less regions. The 'flat field' correction approach (Roberts et al., 1986) assumes that there is an area in the scene that has spectrally neutral reflectance, i.e., the spectrum has little variation with wavelength. The mean spectrum of the "flat field" is then used for the derivation of relative reflectance spectra of other pixels in the scene. In both of these approaches, the derived relative reflectance spectra often have absorption features that are not characteristic of any material in the field or laboratory (Clark & King, 1987). The reason is that the mean spectrum often contains absorption effects of surface materials and is not 100% spectrally neutral (Gao et al, 2009). The use of such mean spectrum can introduce broad absorption

bands in the resulting spectra. The method of empirical line (Conel et al., 1987) requires field measurements of reflectance spectra for at least one bright target and one dark target. The imaging data is then linearly regressed against the field-measured reflectance spectra to derive the gain and offset curves. These gain and offset values are then applied to the whole image for the derivation of surface reflectance for the entire scene. Aspinall et al. (2002) demonstrated that this method produces spectra that are most comparable to characteristic spectra of many materials. For atmospheric corrections over the darker water surfaces, an empirical "cloud shadow" method was developed in the 1990s (Reinersman et al., 1998). This method calculates the differences between the total radiance measured by the sensor over clouded pixels and the neighboring pixels having similar optical properties. The differences are then used for the removal of the nearly identical atmospheric radiance contributions from the measured data. Filippi et al. (2006) used shadows cast by trees and cliffs along coastlines in high spatial resolution (~1 m) hyperspectral imagery for atmospheric corrections. Radiative transfer codes (i.e. LOWTRAN and MODTRAN) can model the effects of scattering in the atmosphere. The RT codes require information on solar and flight geometry as well as certain atmospheric parameters. This is used to generate an atmospheric look-up table (LUT) for all spectral bands. Thus, atmospheric database contains pre-calculated LUTs (i.e. tables of atmospheric transmittance, path radiance etc.) for a wide range of weather conditions (Richter 1996; Staenz & Williams, 1997). Using scattering and transmission properties of the atmosphere, the difference between the radiation leaving the earth and the radiation received at the sensor is modeled by radiative transfer codes having typical atmosphere models for a large number of atmosphere types so as to calculate atmospheric radiance

spectrum on a pixel-by-pixel basis. The surface reflectance is then computed by using the ratio of radiance at the sensor to the model solar irradiance. Roberts et al. (1986) and Moran et al. (1992) have discussed the advantages and shortcomings of empirical and physically based atmospheric correction techniques. Amongst the RT models, 6S code (Vermote et al., 1997) and MODTRAN (Berk et al., 1998) are generally accepted and validated. The 5S code was replaced with 6S code for modeling atmospheric scattering effects. MODTRAN covers the solar and thermal region, thus enabling atmospheric correction for sensors with combined reflective and thermal bands.

Scattering and absorption of water vapor, mixed gases and topographic effects can be corrected using absolute reflectance methods and so they are preferred over relative correction techniques (Nikolakopoulos et. al., 2002) as, they model the atmosphere according to the similar environmental and geographical conditions when the image is acquired. Many researchers have also used combinations of radiative modeling and empirical approaches for the derivation of surface reflectance from hyperspectral imaging data (Boardman, 1998; Goetz et al., 1997).

The first attempt in the direction of RT modeling was through the development of Atmosphere Removal algorithm (ATREM) (Gao et al.,1993). Since then, a number of atmospheric correction algorithms for retrieving surface reflectance from hyperspectral imaging data have come into picture. For e.g. the High-accuracy Atmospheric Correction for Hyperspectral Data (HATCH) (Qu et al., 2003), the Atmosphere CORrection Now (ACORN) (Kruse, 2004), the Fast Lineof- sight Atmospheric Analysis of Spectral Hypercubes (FLAASH) (Adler-Golden et al., 1999), the Imaging Spectrometer Data Analysis System (ISDAS) (Staenz et al., 1998), and a series of Atmospheric and

Topographic Correction (ATCOR) codes (Richter & Schlaepfer, 2002). Till now, atmospheric correction algorithms continue to be refined and improved.

The Air Force Research Laboratory, Space Vehicles Directorate (AFRL/VS) developed a software package, the Fast Line-of-sight Atmospheric Analysis of Spectral Hypercubes (FLAASH) atmospheric correction code which derives its physics-based algorithm from the MODTRAN4 radiative transfer code (Felde et. al., 2003). FLAASH is designed to eliminate atmospheric effects caused by molecular and particulate scattering and absorption from the radiance at the sensor and to obtain reflectance at the surface. The Normalized Optical Depth Derivative (NODD) and atmospheric absorption features are used for an automated wavelength recalibration algorithm in FLAASH. Felde et. al., (2003) verified the use of FLAASH for atmospherically correcting Hyperion data. Griffin & Burke (2003) and Kruse (2004) showed that reflectance retrieved from ATREM, ACORN, and FLAASH are quite comparable.

1.3 STUDY OBJECTIVES

The above-mentioned factors render understanding of data quality issues especially for vegetation assessment. Simultaneously, it is important to establish optimum sensor specifications for future Hyperspectral missions focusing vegetation. Consequently, the objectives of the thesis were formulated as follows:

1. Understanding data quality pertaining to inherent issues, interpretation issues, data redundancy, image classification and atmospheric correction.
2. Establishing optimum spatial and spectral specifications for future hyperspectral sensors with regards to vegetation studies

1.4 OUTLINE OF THESIS

The thesis comprises of five chapters in all. This chapter has included an introduction to the topic of remote sensing with special emphasis on hyperspectral remote sensing and its evolution. It has pointed out the advantages and limitations of hyperspectral sensors in addition to providing an insight to the current applications of hyperspectral data in the field of vegetation studies. It has provided a detailed overview as well as literature survey of the inherent quality issues of the hyperspectral data like band shift, noise, poor band-to-band registration etc. Additionally, it has addressed the important concerns that adversely affect vegetation assessment like atmospheric interferences, band redundancy, use of conventional classifiers etc.

Chapter2 consists of a detailed discussion on the inherent quality issues, with special reference to detection of smile effect, band-to-band registration, scene noise, image distortion, standard range of radiance values, sources of experimental errors including variation with exposure time, effect of inappropriate sampling, effect of leaf stacking, effect of phenology and species and effect of saturation radiance.

Chapter 3 includes a discussion on the importance of atmospheric correction, both through the relative and absolute methods. It has included a discussion on what effect they create on the vegetation spectra. The effect of hyperspectral data redundancy on vegetation analysis is discussed through a number of methods. This understanding was drawn on the basis of classification accuracy. Here, conventional classifiers vs hyperspectral-centric classifiers are studied and reported. Additionally, it has shown the novel technique developed for feature extraction based on image texture

Chapter 4 includes the effect of spatial resolution on vegetation image interpretation. It also includes the effect of spectral resolution on the identification of various kinds of vegetation. Based on this study, optimum sensor definition parameters for vegetation assessment are defined and discussed.

Finally, Chapter 5 consists of conclusions derived from the entire study. This has also included the scope for future study.

References

Adão, T. Hruška, J., Pádua, L., Bessa, J., Peres, E., Morais, R. and João Sousa, J. (2017). Hyperspectral Imaging: A Review on UAV-Based Sensors, Data Processing and Applications for Agriculture and Forestry Remote Sens. 9, 1110; doi:10.3390/rs9111110.

Adler-Golden, S. M., Matthew, M. W., Bernstein, L. S., Levine, R. Y., Berk, A., Richtsmeier, S. C., Acharya, P. K., Anderson, G. P., Felde, G., Gardner, J., Hike, M., Jeong, L. S., Pukall, B., Mello, J., Ratkowski, A., and Burke, H. (1999). Atmospheric correction for shortwave spectral imagery based on MODTRAN4. SPIE Proc. Imaging Spectrometry. 3753, pp. 61-69.

Anderson, J. R., Hardy, E. E., Roach, J. T. and Witmer, R. E. (1976). A land use and land cover classification system for use with remote sensor data. U.S. Geological Service Professional Paper, 964.

Anderson, K. (2005). Temporal variables in calibrating target reflectance: methods, models and applications. PhD. Thesis, University of Southampton, U.K.

Anger, C.D., Babey, S.K., Adamson, R.A. (1990). Anew approach to imaging spectroscopy. Proceedings of SPIE. 72, pp 72-86.

ASD, Products-Software, Analytical Spectral Devices. Accessed: 03/01/07, http://www.asdi.com/, 2006.

Asner, G. P., Boardman, J., Field, C. B., Knapp, D. E., Kennedy B., T., Jones, M. O., & Martin, R. E. (2007). Carnegie airborne observatory: Inflight fusion of hyperspectral imaging and waveform light detection and ranging for three dimensional studies of ecosystems. Journal of Applied Remote Sensing. 1, 013536.

Asner, G.P., Martin, R.E. (2008). Airborne spectranomics: mapping canopy chemical and taxonomic diversity in tropical forests. Front. Ecol. Environ. 7 (5), pp 269–276.

Asner, G.P., Mascaro, J., Muller-Landau, H.C., Vieilledent, G., Rasamoelina, M., van Breugey, M. (2012). A universal airborne LiDAR approach for tropical forest carbon mapping. Oecologia. 168 (4), pp 1147–1160.

Aspinall, R. J. (2002). Use of logistic regression for validation of maps of the spatial distribution of vegetation species derived from high spatial resolution hyperspectral remotely sensed data. Ecological Modelling. 157(2-3), pp 301-312.

Bachmann, C.M., Ainsworth, T.L. and Fusina, R.A. (2005). Exploring manifold geometries in hyperspectral imagers. IEEE Transactions in Geoscience and Remote Sensing. 43 (3), pp 441-454.

Ballanti, L., Blesius, L., Hines, E. and Kruse, B. (2016). Tree Species Classification Using Hyperspectral Imagery: A Comparison of Two Classifiers. Remote Sens. 8, p 445, doi:10.3390/rs8060445.

Bannari, A., Pacheco, A., Staenz, K., McNairn, M., Omari, K. (2006). Estimating and mapping crop residue cover in agricultural lands using hyperspectral and IKONOS images. Remote Sens. Environ. 104, 447–459.

Bannari, A., Staenz, K., Champagne, C. and Khurshid, K.S. (2015). Spatial Variability Mapping of Crop Residue Using Hyperion (EO-1) Hyperspectral Data. Remote Sens. 7, pp 8107-8127, doi:10.3390/rs70608107.

Barnsley, M.J., Settle, J.J., Cutter, M.A., Lobb, D.R. and Teston. (2004). The Proba/CHRIS mission: A low cost smallsat for Hyperspectral, multiangle observation of Earth surface and atmosphere. IEEE Transactions on geoscience and remote sensing. 42, pp 1512-1520.

Barry, P., Seqal, C., and Carman, S. (2001). EO-1 Hyperion science Data User's Guide. TRW Space, Defense and Information Systems. 1 (77), pp 1-65.

Bartley, G.E., Scolnik, P.A. (1995). Plant carotenoids: Pigments for photoprotection, visual attraction, and human health. Plant Cell. 7, 1027–1038.

Beamish, A.L., Coops, N., Chabrillat, S., Heim, B. (2017). A Phenological Approach to Spectral Differentiation of Low-Arctic Tundra Vegetation Communities, North Slope, Alaska. Remote Sens. 9, 1200, doi:10.3390/rs9111200.

Berk, A., Bernstein, L.S., Anderson, G.P., Acharya, P.K., Robertson, D.C., Chetwynd, J.H. and Adler Golden, S.M. (1998). MODTRAN Cloud and multiple scattering

upgrades with application to AVIRIS. Remote Sensing of Environment. 65, pp 367-375.

Bhaskaran, S., Forster, B. and Neal, T. (2001). Integrating airborne hyperspectral sensor data with GIS for hail storm post-disaster management. Proceedings of the 22nd Asian Conference on Remote Sensing, Singapore November 5-9.

Biggar, S., Thome, K.J., Wisniewski, W.T. (2003). Vicarious radiometric calibration of E0-1 sensors by reference to reflectance ground targets. IEEE transaction on geoscience and remote sensing. 41, pp 1174-1179.

Blackburn, G.A. (1999). Relationships between Spectral Reflectance and Pigment Concentrations in Stacks of Deciduous Broadleaves. Remote Sens. Environ. 70, pp 224–237. doi: 10.1016/S0034-4257(99)00048-6.

Boardman, J. W. (1993). Automated spectral unmixing of AVIRIS data using convex geometry concepts. In Summaries 4th JPL Airborne Geoscience Workshop, vol. 1. Pasadena, CA, 1993, 93–26, pp. 11–14.

Boardman, J. W. (1998). Post-ATREM polishing of AVIRIS apparent reflectance data using EFFORT: A lesson in accuracy versus precision. Summaries 7th JPL Airborne Earth Science Workshop.1. Pasadena, CA.

Boardman, J. (2006). Soil erosion science: reflections on the limitations of current approaches. Catena. 68, pp 73–86.

Bruce, L.M. and Jiang, Li. (2001). Wavelets for computationally efficient hyper derivative analysis. IEEE trans. in geo. and remote sensing. 39(7), pp 1540-1546.

Buckingham, R., and Staenz, K. (2008). Review of current and planned civilian space hyperspectral sensors for EO. Canadian Journal of Remote Sensing. 34, pp 187-197.

Campbell, J. B. (2002). Introduction to remote sensing (3rd Ed.). London: Taylor and Francis canopy reflectance indices and discriminant analysis. Crop Science. 35 pp 1400–1405.

Carmona, P.L., Sotoca, J.M., Pla, F., Dias, J.B., Ferrer, C.J. (2013). Effect of denoising in band selection for regression tasks I hyperspectral datasets. IEEE journal of selected topics in applied Earth observations and remote sensing, 6(2-2), pp 473-481.

Ceamanos, X. and Doute, S. (2010). Spectral Smile Correction of CRISM/MRO Hyperspectral Images. IEEE Transactions on Geoscience and Remote Sensing. 48 (11): Doi:10.1109/tgrs.2010.2064326.

Chalker-Scott, L. (1999). Environmental significance of anthocyanins in plant stress responses. Photochem. Photobiol. 1–9.

Chang, C.I. (2002). Target signature constituent mixed pixel classification for hyperspectral imaging. IEEE trans geosc. and rem. sen. 40 (2), pp 1065-1081.

Christian, B. and Krishnayya, N.S.R. (2009). Classification of tropical trees growing in a sanctuary using Hyperion (EO-1) and SAM algorithm. Current Science. 96 (12), pp 1601-1607.

Christophe, E., Leger, D., Mailhes, C. (2005). Quality criteria benchmark for hyperspectral imagery. IEEE Transactions on Geoscien. 43(9).

Clark, R.N. and King, T.V.V. (1987). Causes of spurious features in spectral reflectance data. In Proceedings of the 3rd airborne imaging spectrometer data analysis workshop (G. Vane, Ed) JPL Publication, Pasadena, CA, pp 132-137.

Clark, R.N. and Swayze, G.A. (1995). Mapping minerals, amorphous materials, environmental materials, vegetation, water, ice and snow, and other materials: The USGS Tricorder Algorithm. Summaries of the Fifth Annual JPL Airborne Earth Science Workshop, January 23- 26, R.O. Green, Ed., JPL Publication 95-1, p. 39-40.

Clark, R.N. (1999). Spectroscopy of Rocks and Minerals, and Principles of Spectroscopy. In Renz, Andrew N. (ed), Remote Sensing for the Earth Sciences: Manual of Remote Sensing (3rd ed.), Vol 3. New York: John Wiley & Sons, pp. 3-58.

Clark, R.N., Swayze, G.A. Livo, K.E. Kokaly, R.F. Sutley, S.J. Dalton, J.B. McDougal, R.R. and Gent, C.A. (2003). Imaging Spectroscopy: earth and planetary remote

sensing with the USGS Tetracorder and expert systems, Journal of Geophys Research. 18(E12), p 5131.

Clark, M. L., Roberts, D. A. and Clark, D. B. (2005). Hyperspectral discrimination of tropical rain forest tree species at leaf to crown scales. Remote Sensing of Environment. 96(3-4), pp 375-398.

Cochrane, M. A. (2000). Using vegetation reflectance variability for species level classification of hyperspectral data. International Journal of Remote Sensing. 21(10), pp 2075-2087.

Cochrane, M.A. (2010). Using vegetation reflectance variability for species level classification of hyperspectral data. International Journal of Remote Sensing. 21, pp 2075–2087.

Coley, P.D., Barone, J.A. (1996). Herbivory and plant defences in tropical forests. Annual Review of Ecology and Systematics. 27, pp 305–335.

Colwell, R.N. (1983). Manual of remote sensing-second edition. American society of Photogrammetry, Falls church.

Conel, J.E., Green, R.O., Vane, G., Bruegge, C.J., Alley, R.E. and Curtiss, B.J. (1987). Airborne imagig spectrometer-2: radiometric, spectral characteristics and comparison of ways to compensate for atmosphere. Proceedings of SPIE, 8-34, pp 140-157.

Corner, B.R., Narayanan, R.M. and Reichenbach, S.E. (2003). Noise estimation in remote sensing imagery using data masking. International Journal of Remote Sensing. 24 (4), pp 689-702. Doi:10.1080/01431160210164271.

Corson, M.R., Korwan, D.R., Lucke, R.L., Snyder, W.A., Davis, C.O. (2008). The hyperspectral imager for coastal oceans (HICO) on the international space station. IEEE proceedings of the international geoscience and remote sensing symposium. 978-1-4244-2808-3/08.

Curran, P. (1989). Remote sensing of foliar chemistry. Remote Sens. Environ. 30, pp 271–278.

Curran, P. J., Dungan, J. L. and Gholz, H. L. (1990). Exploring the relationship between reflectance red edge and chlorophyll content in slash pine. Tree Physiology. 7 pp 33-48.

Dadon, A., Ben-Dor, E. and Karnieli, A. (2010a). Use of Derivative Calculations and Minimum Noise Fraction Transform for Detecting and Correcting the Spectral Curvature Effect (Smile) in Hyperion Images. IEEE Transactions on Geoscience and Remote Sensing. Doi:0.1109/TGRS.2010.2040391.

Dadon, A., Karnieli, A., Ben-Dor, E. (2010b). Detecting and correcting the curvature effect (smile) in Hyperion images by use of MNF. proceedings of 'Hyperspectral 2010 Workshop', Frascati, Italy, 17–19 March 2010.

Datt B. (1999). A New Reflectance Index for Remote Sensing of Chlorophyll Content in Higher Plants: Tests using Eucalyptus Leaves. J. Plant Physiol. 154 pp 30–36. doi: 10.1016/S0176-1617(99)80314-9.

Daughtry, C.S.T., Walthall, C.L., Kim, M.S., De Colstoun, E.B., McMurtrey, J.E. (2000). Estimating corn leaf chlorophyll concentration from leaf and canopy reflectance. Remote Sens. Environ.74 pp 229–239. doi: 10.1016/S0034-4257(00)00113-9.

Daughtry, C.S.T., Hunt, E.R., Jr, Doraiswamy, P.C., McMurtrey, J.E. (2005). Remote sensing the spatial distribution of crop residues. Agron. J. 97, pp 864-871.

Davis, C.O.; Kappus, M.; Bowles, J.; Fisher, J.; Antoniades, J.; Carney, M. (1999). Calibration, characterization and first results with the ocean PHILLS hyperspectral imager. Proc. SPIE 1999, 3753, 160–168.

Dennison, P.E., Roberts, D.A. (2003). The effects of vegetation phenology on endmember selection and species mapping in southern California chaparral Remote Sensing of Environment. 87, pp 295–309.

Du, Q. and Chang, C.I. (2001). A linear constrained dist. based discriminant analysis for hyperspectral image classification. Pattern recognition. 34(2), pp 361-373.

Duggin, M.J. & Philipson, W.R. (1982). Field measurement of reflectance, some major considerations. Applied optics. 21 (15), pp 2833-2840.

Eitel, J.U.H., Gessler, P.E., Smith, A.M.S., Robberecht, R. (2006). Suitability of existing and novel spectral indices to remotely detect water stress in Populus spp. For. Ecol. Manag. 229, pp 170–182. doi: 10.1016/j.foreco.2006.03.027.

Eklundh, L. and Singh, A. (1993). A comparative analysis of standardized and unstandardized principal component analysis in remote sensing. Int J of Remote Sens. 14 (7), pp 1359-1370.

Ellis, J. (2003). Hyperspectral imaging technologies key for oil seep/oil-impacted soil detection and environmental baselines. Environmental Science and Engineering. http://www.esemag.com/0503/index.html.

Engel, J.L. and Weinstein, O. (1983). Thematic mapper, an overview. IEEE Trans. in Geosc. and Remote Sens. 21(3), pp 258-265.

Fairweather, S., Potter, C., Crabtree, R., Li, S. (2012). A comparison of multispectral ASTER and hyperspectral AVIRIS multiple endmember spectral mixture analysis for sagebrush and herbaceous cover in Yellowstone. Photogrammetric Engineering and Remote Sensing 78, 23–33.

Felde, G.W. et. al. (2003). Analysis of Hyperion data with FLAASH atmospheric correction algorithm. IGARSS, Toulouse, FR.

Feng, Y. and Xiang, Y. (2002). Mitigation of spectral mis-registration effects in imaging spectrometers via cubic spline interpolation. Opt. Express. 16(20), pp 210-221.

Feret, J.-B., and G. P. Asner. (2014). Mapping tropical forest canopy diversity using high-fidelity imaging spectroscopy. Ecol. Appl. 24, pp 1289–1296.

Field, C., Mooney, H.A. (1983). Leaf age and seasonal effects on light, water, and nitrogen use efficiency in a California shrub. Oecologia. 56, pp 348–355.

Filella, I., Serrano, L., Serra, J. and Penuelas, J. (1995). Evaluating wheat nitrogen status with canopy reflectance indices and discriminant analysis. Crop Science. 35 pp 1400–1405.

Filippi, A.M., Carder, K., Davis, C.O. (2006). Vicarious calibration of ocean PHILLS hyperspectral sensor using a coastal tree shadow method. Geophysical Research letters. 33, L22605, DOI:10.1029/2006GL027023.

Foody, G. (2004). Thematic map comparison: Evaluating the statistical significance differences in classification accuracy. Photogramm. Eng. Remote Sens. 70, pp 627–633.

Fox, N.P. (2001). Traceability to SI for EO missions. CEOS WGCV Cal/Val Newsletter. 9, pp 1-9.

Fukunaga, K. (1990). Introduction to Statistical Pattern Recognition. Academic Press Inc., San Diego, California.

Gamon, J. A. and Surfus, J. S. (1999). Assessing leaf pigment content and activity with a reflectometer. New Phytologist. 143(1) pp 105-117.

Gamon, J.A., Berry, J.A. (2012). Facultative and constitutive pigment effects on the Photochemical Reflectance Index (PRI) in sun and shade conifer needles. Isr. J. Plant Sci. 60, pp 85–95.

Gao, B.C., Heidebrecht, K.H. and Goetz, A. F. H. (1993). Derivation of scaled surface reflectances from AVIRIS data. Remote Sensing of Environment. 44, pp. 165-178.

Gao, B. (1996). NDWI—A normalized difference water index for remote sensing of vegetation liquid water from space. Remote Sens. Environ. 58, pp 257–266. doi: 10.1016/S0034-4257(96)00067-3.

Gao, B.C., Monets, M, Davis, C. (2004). Refinement of wavelength calibrations of hyperspectral imaging data using a spectrum matching techniques. Remote Sensing of Environment. 90 (4): 424-433.

Gao, B.C., Davis, C. and Goetz, A. (2006). A Review of Atmospheric Correction Techniques for Hyperspectral Remote Sensing of Land Surfaces and Ocean Color. Geoscience and Remote Sensing Symposium pp. 1979-1981.

Gao, B. C., Montes, M. J., Davis, C. O., & Goetz, A. F. (2009). Atmospheric correction algorithms for hyperspectral remote sensing data of land and ocean. Remote Sensing of Environment. 113, pp S17-S24.

Gates, D.M., Keegan, H.J., Schleter, J.C. and Victor R. (1965). Spectral Properties of Plants. Applied Optics, 4 (1).

Gausman, H. W. et al. (1971). The leaf mesophylls of twenty crops, their light spectra and optical and geometrical parameters. Spectral Survey of irrigated region crops and soils. Annual report, Dept. of Agriculture, Weslaco, Texas.

Gausman, H. W. (1974). Leaf reflectance of near-infrared. Photogrammetric Engineering. 40, pp 183–191.

Ghamisi, P. (2015). Spectral and Spatial Classification of Hyperspectral Data A Thesis Presented in Partial Fulfillment of the Requirements for the Degree Doctor of Philosophy in Electrical and Computer Engineering at the University of Iceland. ISBN 978-9935-9243-3-9.

Gitelson, A.A., Merzlyak, M.N. and Lichtenthaler, H.K. (1996). Detection of Red Edge Position and Chlorophyll Content by Reflectance Measurements near 700 nm. J. Plant Physiol. 148, pp 501–508. doi: 10.1016/S0176-1617(96)80285-9.

Gitelson, A.A. and Merzlyak M.N. (1997). Remote estimation of chlorophyll content in higher plant leaves. Int. J. Remote Sens. 18, pp 2691–2697. doi: 10.1080/014311697217558.

Gitelson, A.A., Gritz, Y. and Merzlyak, M.N. (2003). Relationships between leaf chlorophyll content and spectral reflectance and algorithms for non-destructive chlorophyll assessment in higher plant leaves. J. Plant Physiol. 160, pp 271–282. doi: 10.1078/0176-1617-00887.

Goetz, A. F. H., Rowan, L. C. and Kingston, M. J. (1982). Mineral identification from orbit – initial results from the shuttle multispectral infrared radiometer. Science, pp 218:1020–1024.

Goetz, A. F. H., Vane, G., Solomon, J. E. and Rock, B. N. (1985). Imaging spectrometry for Earth remote sensing. Science. 228, pp. 1147–1153.

Goetz, A. F.H. and Boardman, J.W. (1997). Atmospheric Corrections: On Deriving Surface Reflectance from Hyperspectral Imagers. In Descour, Michael R. and Shen, S.S. (eds.), Imaging Spectrometry III: Proceedings of SPIE. 3118, pp 14-22.

Goodenough, D. G., Dyk, A., Niemann, K. O., Pearlman, J. S., Chen, H., Han, T., Murdoch, M., and West, C. (2003). Processing Hyperion and ALI for forest classification. IEEE Trans. Geosci. Remote Sens. 41(6), pp 1321-1331.

Goodin, D.G., Gao, J. and Henebry, G.M. (2004). The Effect of Solar Illumination Angle and Sensor View Angle on Observed Patterns of Spatial Structure in Tallgrass Prairie. IEEE transactions on geoscience and remote sensing. 42 (1).

Green, A. A., Berman, M., Switzer, P., and Craig, M.D. (1988). A Transformation for Ordering Multispectral Data in Terms of Image Quality with Implications for Noise Removal. IEEE Transactions on Geoscience and Remote Sensing.26, pp 65-74.

Green, R. O., Pavri, B., Faust, J. and Williams, O. (1999). AVIRIS radiometric laboratory calibration, inflight validation, and a focused sensitivity analysis in 1998. In Proc. 8th JPL Airborne Earth Science Workshop. 99–17, pp. 161–175. Pasadena, CA.

Griffin, M.K. and Burke, H-H.K. (2003). Compensation of Hyperspectral data for atmospheric effects. Lincoln Laboratory Journal. 14 (1), pp 29-53.

Guanter, L., Kaufmann, H., Foerster, S., Brosinsky, A., Wulf, H., et al. (2016). EnMAP Science Plan—Environmental Mapping and Analysis Program; Technical Report; GFZ Data Services: Potsdam, Germany.

Han, T. and Goodenough, D.G. (2008). Noise reduction of hyperspectral remotely sensed imagery: A Nonlinear dynamical system approach. http://www.securecms.com/igarss2008/abstracts/pdfs/1514.pdf.

Hoffer, R. M., and Johannsen, C. J. (1969). Ecological Potentials in Spectral Signature Analysis. In: Johnson, P. (ed). Remote Sensing in Ecology. Chapter 1, 1-16. University of Georgia Press, Athens, Georgia.

Hollinger, A., Gray, L. H., Gower, J., Edel, H.R. (1987). The Fluorescence Line Imager: An Imaging Spectrometer for Ocean and Land Remote Sensing Article in

Proceedings of SPIE - The International Society for Optical Engineering 834:2-11 DOI: 10.1117/12.942277.

Homma, K., Vamamoto, H. and Iwata, V. (2000). A study on image restoration for airborne cameras. International Archives of Photogrammetry and Remote Sensing. xxxiii (b7), Amsterdam.

http://aviris.jpl.nasa.gov/html/aviris.overview.html.

https://directory.eoportal.org.web.eoportal.airbornesensors.aviris.htm.

https://earthdata.nasa.gov.

Huang, R. (2005). Band Selection Based on Feature Weighting for Classification of Hyperspectral Data. IEEE Geoscience and Remote Sensing Letters. 2(2).

Hueni, A., Damm, A., Kneubuehler, M., Schl¨apfer, D. and Schaepman, M. (2016). Field and airborne spectroscopy cross-validation—Some considerations. IEEE J. Sel. Topics Appl. Earth Observ. Remote Sens. 99, pp. 1–19.

Hughes, G. (1968). On the mean accuracy of statistical pattern recognizers. IEEE Trans. Inf. Theory. 14, pp 55–63.

Iqbal, M. (1983). An Introduction to Solar Radiation. Academic Press, Toronto, ON, Canada.

Jacobsen, A., Heldebrecht, K.B. and Goetz, A. F.H. (2000). Assessing the Quality of the Radiometric and Spectral Calibration of CASI Data and Retrieval of Surface Reflectance Factors. Photogrammetric Engineering & Remote Sensing. 66(9), pp. 1083-1091.

Jensen, J. R. (2005). Introductory Digital Image Processing: A Remote Sensing Perspective. Prentice Hall, Upper Saddle River, NJ.

Jimenez, L.O., Landgrebe, D. A. (1998). Supervised classification in high-dimensional space: Geometrical, statistical, and asymptotical properties of multivariate data. IEEE Transactions on Systems Man and Cybernetics Part C (Applications and Reviews). 28(1), pp 39 - 54 · DOI: 10.1109/5326.661089.

Joseph, G. (2005). Fundamentals of Remote Sensing. 2nd Edition, Universities Press, ISBN-978-8173715358

Jupp, D. L. B., Datt, B., McVicar, T. R., Van Niel, T. G., Pearlman, J. S.J, Lovell, L. and King, E. A. (2002). Improving the Analysis of Hyperion Red-Edge Index from an Agricultural area in SPIE's Third International Asia-Pacific Remote Sensing symposium, Hangzhou, China.

Jupp, D.L.B., Datt, B., Ovell, J., Campbell, S., King, E.A. (2002). Discussions around Hyperion data: background notes for the Hyperion data users workshop, CSIRO, Earth observation centre, Canberra.

Kaufman, Y. J., and Sendra, C. (1988). Algorithm for automatic atmospheric correction to visible and near-IR satellite imagery. Int. J. Remote Sens. 9, pp 1357–1381.

Kerekes, J.P. and Landgrebe, D.A. (1991). An analytical model of Earth-observational remote sensing systems. IEEE Transactions on Systems, Man, and Cybernetics. 21(1), pp 125 – 133.

Khurshid, K.S., Staenz, K., Sun, L., Neville, R., White, H.P., Bannari, A., Champagne, C.M., Hitchcock, R. (2006). Pre-processing of EO-1 Hyperion data. Canadian journal of remote sensing. 32 (2), pp 84-97.

Kimes, D. S. (1983). Dynamics of directional reflectance factor distributions for vegetation canopies. Appl. Opt. 22, pp 1364-1372.

Kimes, D. S. and Deering, D. W. (1992). Remote sensing of surface hemispherical reflectance (albedo) using pointable multispectral imaging Spectroradiometers. Remote Sensing of Environment. 39(2).

Klancnik, K., Gaberščik, A. (2016). Leaf spectral signatures differ in plant species colonising habitats along a hydrological gradient. J. Plant Ecol. 9, pp 442–450.

Knipling, E. B. (1970). Physical and physiological basis for the reflectance of visible and near-infrared radiation from vegetation. Remote Sensing of Environment. 1, pp 155-159.

Kruse, F.A. (1988). Use of airborne imaging spectrometer data to map minerals associated with hydrothermally altered rocks in the Northern Grapevine Mountains, Nevada and California. Remote Sens. Environ. 24(1), pp. 31–51.

Kruse, F.A., Kierein-Young, K. S. and Boardman, J. W. (1990). Mineral mapping at Cuprite, Nevada with a 63 channel imaging spectrometer. Photogramm. Eng. Remote Sens. 56(1), pp 83–92.

Kruse, F. A. and Lefkoff, A. B. (1993). Knowledge-based geologic mapping with imaging spectrometers. Remote Sens. Rev.8, pp 3–28.

Kruse, F. A., Lefkoff, A. B., Boardman, J.B., Heidebrecht, K. B., Shapiro, A. T., Barloon, P. J. and Goetz, A. F. H. (1993). The spectral image processing system (SIPS)—Interactive visualization and analysis of imaging spectrometer data. Remote Sens. Environ. 44, pp 145–163.

Kruse, F.A., Boardman, J.W. and Huntington, J.F. (2003). Comparison of Airborne Hyperspectral Data and EO-1 Hyperion for Mineral Mapping. IEEE Transactions On Geoscience and Remote Sensing. 41(6).

Kruse, F.A. (2004). Comparison of ATREM, ACORN, and FLAASH Atmospheric Corrections using Low-Altitude AVIRIS Data of Boulder, Colorado. 13th JPL Airborne Geoscience Workshop, Pasadena, CA.

Kumar, L, Schmidt, K., Dury, S., Skidmore, A. (2001). Imaging Spectrometry and Vegetation Science. In van der Meer, F.D. and de Jong, S.M. (eds.). Imaging Spectrometry: Basic Principles and Prospective Applications, Dordrecht: Kluwer Academic Publishers, pp 111-155.

Landgrebe, D. (1997). On information extraction principles for hyperspectral data. http://dynamo.ecn.purdue.edu/~landgreb/whitepaper.pdf.

Landgrebe, D. A. (2003). Signal Theory Methods in Multispectral Remote Sensing, Hoboken, NJ: Wiley.

Lee, C. and Landgrebe, D.A. (1993). Analyzing High Dimensional Multispectral Data. IEEE Transactions on Geoscience and Remote Sensing. 31(4), pp 792-800.

Lelégard, L., Brédif, M., Vallet, B., Boldo, D. (2010). Motion blur detection in aerial images shot with channel-dependent exposure time. In: Paparoditis N., Pierrot-Deseilligny M., Mallet C., Tournaire O. (Eds), IAPRS, Vol. XXXVIII, Part 3A – Saint-Mandé, France.

Li, J., Bioucas-Dias, J.M. and Plaza, A. (2013). Spectral–spatial classification of hyperspectral data using loopy belief propagation and active learning. IEEE Trans. Geosci. Remote Sens. 51 (2), pp 844–856.

Liang, S., Fallah-Adl, H., Kalluri, S., Jaja, J., Yoram, J. K., and Townshend, J. R. G. (1997). An operational atmospheric correction algorithm for Landsat Thematic Mapper imagery over land. J. Geophys. Res. 102(14) pp 173–186.

Liang S. (2004). Quantitative remote sensing of land surfaces. Hoboken NJ, John Wiley and sons.

Liao, L., PJarecke, D., Gleichauf, T. Hedman. (2000). Performance characterization of the Hyperion imaging spectrometer instrument. Proceedings of SPIE. 4135, pp 264-275.

Lodha, S.P.and Kamlapur, S.M. (2014). Dimensionality Reduction Techniques for Hyperspectral Images International Journal of Application. 3(10).

Lord, D., Desjardins, R. L. and Dubé, P.A. (1988). Sun-angle effects on the red and near infrared Reflectances of five different crop canopies. Canadian Journal of Remote Sensing. 14 (1).

Luo, B. and Chanussot, J. (2009). Hyperspectral Image Classification Based On Spectral and Geometrical Features. IEEE transactions on geoscience and remote sensing.

Lyon, R.G. (2004). Understanding Digital Signal Processing, Prentice Hall, New Jersey.

Maksymowych, R. (1973). Analysis of leaf development. Cambridge, UK: Cambridge University Press.

Manjunath, K. R., Dutta, S., Singh, Rimjhim Bhatnagar and Panigrahy, S. (2012). Crop Parameter Retrieval using Ground Spectral Data, Investigations on Hyperspectral

Remote Sensing Applications (Compendium of Project Report and Scientific Investigations), Scientific Report, SAC/EPSA/HYPER/SR/2012/01.

Marconcini, M., Camps-Valls, G., Bruzzone, L. (2009). A composite semisupervised SVM for classification of hyperspectral images. IEEE Geoscience and Remote Sensing Letters. 6 (2), pp 234–238.

Meroni, M., Colombo, R., & Panigada, C. (2004). Inversion of a radiative transfer model with hyperspectral observations for LAI mapping in poplar plantations. Remote Sensing of Environment. 92, pp 195-206.

Merton, R. and Huntington, J. (1999). Early simulation of the ARIES-1 satellite sensor for multi-temporal vegetation research derived from AVIRIS. In Summaries of the Eight JPL Airborne Earth Science Workshop, 9–11 February, 299–307. Pasadena, CA: JPL Publication 99-17.

Milton, E. J. (1987). Principles of field spectroscopy. International Journal of Remote Sensing. 8, pp 1807-1827.

Milton, E. J., Schaepman, E. J., Anderson, K., Kneub¨uhler, M. and Fox, N. (2009). Progress in field spectroscopy. Remote Sens. Environ. 113, pp. 92–109.

Mobasheri, M.R. and Fatemi, S.B. (2013). Leaf Equivalent Water Thickness assessment using reflectance at optimum wavelengths. Theoretical and Experimental Plant Physiology. 25(3), pp 196-202.

Moran, M.S., R.D. Jackson, P.N. Slater, and P.M. Teillet. (1992). Evaluation of simplified procedures for retrieval of land surface reflectance factors from satellite sensor output. Remote Sensing of Environment. 41, pp169-184.

Moran, J.A., Mitchell, A.K., Goodmanson, G., Stockburger, K.A. (2000). Differentiation among effects of nitrogen fertilization treatments on conifer seedlings by foliar reflectance: a comparison of methods. Tree Physiology. 20, pp 1113–1120.

Moran, M. S., Bryant, R., Thome, K., Ni, W., Nouvellon, Y., Gonzalez-Dugo, M. P., et al. (2001). A refined empirical line approach for reflectance factor retrieval from Landsat-5 TM and Landsat-7 ETM+. Remote Sensing of Environment. 78, pp 71 – 82.

Mouroulis, P., Green, R. O., and Chrien, T. G. (2000). Design of Pushbroom imaging spectrometers for optimum recovery of spectroscopic and spatial information. Appl. Opt. 39(13), pp 2210-2220.

Muhammed, H.H. (2005). Hyperspectral Crop Reflectance Data for characterising and estimating Fungal Disease Severity in Wheat. Biosystems Engineering. 91(1), pp 9-20.

Mutanga, O. and Skidmore, A.K. (2004). Narrow band vegetation indices overcome the saturation problem in biomass estimation. Int. J. Remote Sens. 25, pp 3999–4014. doi: 10.1080/01431160310001654923.

Myers, D. (1997). Radiometric Instrumentation and Measurements Guide for Photovoltaic Performance Testing. National Renewable Energy Laboratory, Golden, Colorado. NREL/TP-560-21774.

Neuwirthová, E., Hotáková, Z.L. and Albrechtová, J. (2017). The Effect of Leaf Stacking on Leaf Reflectance and Vegetation Indices Measured by Contact Probe during the Season. Sensors (Basel). 17(6), p 1202. doi: 10.3390/s17061202.

Neville, R. A., Sun, L., and Staenz, K. (2003). Detection of spectral line curvature in imaging spectrometer data. Proc. SPIE 5093, pp144-154.

Neville, R.A, Sun, L., Staenz, K. (2008). Spectral calibration of imaging spectrometers by atmospheric absorption feature matching. Can. J. Remote Sens. 34, pp 29–42.

Nicholson, K.C., Sears, M., Robin, A. (2013). Evaluation of bands containing spectrally correlated noise in hyperspectral imagery. 5th workshop on hyperspectral image and signal processing-evolution in remote sensing (WHISPERS). DOI:10.1109/WHISPERS/2013.8080732.

Nikolakopoulos, K.G., Vaiopoulos, D.A., Skianis, G.A. (2002). A Comparative Study of Different Atmospheric Correction Algorithms Over An Area With Complex Geomorphology in Western Peloponnese, Greece, Geoscience and Remote Sensing Symposium, IGARSS '02, IEEE International, 4, pp. 2492 –2494.

Orych, A., Walczykowski, P., Jenerowicz, A., Zdunek, Z. (2014). Impact of the Cameras Radiometric Resolution on the Accuracy of Determining Spectral Reflectance

Coefficients. International Archives of the Photogrammetry, Remote Sensing and Spatial Information Sciences. XL-1, pp 347-349.

Ose, K., Corpetti, T. and Demagistri, L. (2017). Multispectral Satellite Image Processing. In Nicolas Baghdadi and Mehrez Zribi (Ed). Optical Remote Sensing of Land Surface Techniques and Methods.

Panigrahy, S., Ray, S.S., Manjunath, K.R., Singh, Rimjhim Bhatnagar, Singh, C.P. and Kumar, T. (2011). Data Quality Evaluation of Airborne Imaging Spectrometer (AIMS), EOAM/SAC/ABHG/HA/SN/01/2011.

Pantin, F., Simonneau, T., Muller, B. (2012). Coming of leaf age: control of growth by hydraulics and metabolics during leaf ontogeny. New Phytologist. 196, pp 349–366.

Pearlman, J., Carman, S., Lee, P., Liao, L. and Segal, C. (1999). Hyperion imaging spectrometer on the new millennium program Earth Orbiter-1 system. In Proc. Int. Symp. Spectral Sensing Research (ISSSR), Systems and Sensors for the New Millennium.

Pearlman, J.S., Barry, P.S., Segal, C.C., Shepanski, J., Beiso, D. and Carman, S.L. (2003). Hyperion-a space based imaging spectrometer. IEEE, Tran geoscience and Remote Sensing. 41(6), pp 1160-1173.

Peterson, J., Vignola, F., Habte, A. and Sengupta, M. (2017). Developing a Spectroradiometer data uncertainty methodology. Solar Energy. 149, pp 60–76.

Pfitzner, K.; Bollhöfer, A.; Esparon, A.; Bartolo, B.; Staben, G. Standardized spectra (400–2500 nm) and associated metadata: An example from northern tropical Australia. (2010). In Proceedings of IEEE International Geoscience and Remote Sensing Symposium, Honolulu, Hawaii, USA, 25–30 July 2010.

Phillips, R.D., Watson, L.T. Blinn, C. E. and Wynne, R.H. (2008). An adaptive noise reduction technique for improving the utility of hyperspectral data. Pecora 17 – The Future of Land Imaging...Going Operational November 18 – 20, 2008, Denver, Colorado.

Plaza, A., Benediktsson, J.A., Boardman, J.W., Brazile, J., Bruzzone, L., Camps-Valls, G., Chanussot, J., Fauvel, M., Gamba, P., Gualtieri, A. (2009). Recent advances in techniques for hyperspectral image processing. Remote Sens. Environ. 113, pp 110–122.

Purkis, S.J., and Klemas, V.V. (2011). Remote Sensing and Global Environmental Change.

Qu, Z., Kindel, B.C. and Goetz, A.F.H. (2003). The high accuracy atmospheric correction for hyperspectral data (HATCH) model. IEEE, transaction geoscience and remote sensing. 41, pp 1223-1231.

Ranjitha, G. and Srinivasan, M. R. (2014). Hyperspectral radiometry for the detection and discrimination of damage caused by sucking pests of cotton. Current Biotica. 8(1), pp 5-12, 2014.

Ranson, K. J., Daughtry, C. S. T., Biehl, L. L. and Bauer, M. E. (1985). Sun-View Angle Effects on Reflectance Factors of Corn Canopies. Remote Sensing of Environment. 18, pp147-161. ISSN 0973-4031.

Rast, M., Baret, E, Menend, M., Schimel, D., Verstraete, M.M., Mauser, W, Miller, J., & Schaepman, M. (2001). SPECTRA - Surface Processes and Ecosystem Changes Through Response Analysis ESA, Noordwijk.

Reinersman, P.N., Carder, K., Chen, F.I.R. (1998). Satellite-Sensor Calibration Verification with the Cloud-Shadow Method. Applied Optics. 37(24), pp 5541-9.

Richardson, A. D. and Berlyn, G. P. (2002). Changes in foliar spectral reflectance and chlorophyll fluorescence of four temperate species following branch cutting. Tree Physiology. 22, pp 499-506.

Richter, R. (1996). A spatially adaptive fast atmospheric correction algorithm. Int. J. Remote Sens. 17, pp 1201–1214.

Richter, R., and Schläpfer, D. (2002). Geo-atmospheric processing of airborne imaging spectrometry data. Part 2: atmospheric / topographic correction. Int. J. Remote Sensing. 23, pp 2631-2649.

Roberts, D. A., Yamaguchi, Y., & Lyon, R. J. P. (1986). Comparison of various techniques for calibration of AIS data. Proceedings of the 2nd AIS workshop. JPL Publication. 86 (35). Pasadena, CA.

Rocchini, D., Balkenhol N., Carter G., Foody G., Gillespie T., He K., ⋯ Neteler M. (2010). Remotely sensed spectral heterogeneity as a proxy of species diversity: Recent advances and open challenges. Ecological Informatics. 5, pp 318–329.

Ross, J. (1981). The Radiation Regime and Architecture of Plant Stands. Junk, The Hague.

Royer, A., Vincent, P. and Bonn, F. (1985). Evaluation and Correction of Viewing Angle Effects on Satellite Measurements of Bidirectional Reflectance. Photogrammetry Nigerian. 51 (12), pp. 1899-1914.

Running, S. W., Justice, C.O., Salomonson, V., et al. (1994). Terrestrial remote sensing science and algorithms planned for EOS/MODIS. Int. J. Remote Sens. 17, pp 3587—3620.

Salehia, B. and Valadanzoej, M.J. Wavele-based Reduction of Hyperspectral Imagery

Savitzky, A. and Golay, M. J. E. (1964). Smoothing and differentiation of data by simplified least-squares procedures. Analytical Chemistry. 36(8), pp 1627-1639.

Schaepman, M.E. (2007). Spectrodirectional remote sensing: From pixels to processes. International Journal of Applied Earth Observation and Geoinformation. 9(2), pp 204-223. DOI: https://doi.org/10.1016/j.jag.2006.09.003.

Schaepman M.E., Ustin, S.L., Plaza, A.J., Painter, T.H., Verrelst, J., Liang, S. (2009). Earth system science related imaging spectroscopy—An assessment. Remote Sensing of Environment. 113, pp S123–S137.

Schiefer, S., Hostert, P., Damm, A. Analysis of view-angle effects in hyperspectral data of urban areas. http://www.isprs.org/proceedings/XXXVI/8-W27/schiefer.pdf.

Schla¨pfer, D., Borel, C. C., Keller, J. and Ittem, K. I. (1998). Atmospheric precorrected Verential absorption technique to retrieve columnar water vapor. Remote Sensing of Environment. 65, pp 353–366.

Schmidt, K. S. and Skidmore, A. K. (2004). Smoothing vegetation spectra with wavelets. International Journal of Remote Sensing. 25(6), pp 1167-1184.

Schmidt, K. S., Skidmore, A. K., Kloosterman, E. H., Van Oosten, H., Kumar, L. and Janssen, J. A. M. (2004). Mapping Coastal Vegetation Using an Expert System and Hyperspectral Imagery. Photogrammetric Engineering and Remote Sensing. 70(6), pp 703-715.

Seelig, H.D., Hoehn, A., Stodieck, L.S., Klaus, D.M., Adams, W.W. and Emery, W.J. (2008). The assessment of leaf water content using leaf reflectance ratios in the visible, near-, and short-wave-infrared. International Journal of Remote Sensing. 29 (13). https://doi.org/10.1080/01431160701772500.

Serpico, S. B., Member, S., & Moser, G. (2007). Extraction of spectral channels from hyperspectral images for classification purposes. IEEE Transactions on Geoscience and Remote Sensing. 45(2), pp. 484-495.

Shaw, G. and Manolakis, D. (2002). Signal processing for hyperspectral image exploitation. IEEE Signal Process. Mag. 19, pp. 12 – 16.

Shippert, P. (2004). Why use hyperspectral imagery? Photogramm. Eng. Remote Sens. 70, pp 377–396.

Singh, Rimjhim Bhatnagar, Mahtab, A. and Ajai. (2009). Target Separability analysis for Resourcesat-1 AWiFS data. Journal of Geomatics. 3 (1).

Singh, Rimjhim Bhatnagar, Ray, S.S., Bal, S.K., Sekhon, B.S., Gill, G.S. and Panigrahy, S. (2013). Crop Residue Discrimination Using Ground-Based Hyperspectral Data. Journal of the Indian Society of Remote Sensing. 41(2), pp 301–308.

Singh, Rimjhim Bhatnagar, Ray, S.S. and Sharma, A.C. (2015). Feature Extraction of Hyperspectral Imaging Data using Texture Analysis. Journal of Geomatics. 9(1).

Slater, P. N., Biggar, S. F., Holm, R. G., Jackson, R. D., Mao, Y., Moran, M. S., et al. (1987). Reflectance- and radiance-based methods for the in-flight absolute calibration of multispectral scanners. Remote Sensing of Environment. 22, pp 11-37.

Slaton, M.R., Hunt, E.R. and Smith, W.K. (2001). Estimating near-infrared leaf reflectance from leaf structural characteristics. Am. J. Bot. 88, pp 278–284. doi: 10.2307/2657019.

Smith, K. L., Steven, M. D. and Colls, J. J. (2004). Use of hyperspectral derivative ratios in the red-edge region to identify plant stress responses to gas leaks. Remote Sensing of Environment. 92(2), pp 207-217.

Smith, M.L., Ollinger, S.V., Martin, M.E., Aber, J.D., Hallett, R.A., Goodale, C.L. (2002). Direct estimation of aboveground productivity through hyperspectral remote sensing of canopy nitrogen. Ecological Applications. 12, pp 1286–1302.

Sobhan, M.I. (2007). Species discrimination from a hyperspectral perspective. International Institute for Geo-Information Science & Earth Observation. Enschede, the Netherlands (ITC). ITC Dissertation Number: 150. ISBN: 978-90-8504-809-1.

Staenz, K., Williams, D.J. (1997). Retrieval of Surface Reflectance from Hyperspectral Data Using a Look-Up Table Approach. Can. J. Remote Sens. 23, pp 354–368.

Staenz, K., Szeredi, T., Schwarz, J. (1998). ISDAS A system for processing and analyzing hyperspectral data. Can. J. Remote Sens. 42, pp 99–113.

Staenz, K., Neville, R.A., Clavette, S., Hitchcock, R. (2002). Retrieval of surface reflectance from Hyperion radiance data. Geoscience and Remote Sensing Symposium, 2002. IGARSS '02. 2002 IEEE International, Volume: 3. DOI: 10.1109/IGARSS.2002.1026135.

Steinberg, A., Chabrillat, S., Stevens, A., Segl, K., Foerster, S. (2016). Prediction of Common Surface Soil Properties Based on Vis-NIR Airborne and Simulated EnMAP Imaging Spectroscopy Data: Prediction Accuracy and Influence of Spatial Resolution. Remote Sens. 8, p 613.

Steyn, W.J., Wand, S.J.E., Holcroft, D.M., Jacobs, G. (2002). Anthocyanins in vegetative tissues: A proposed unified function in photoprotection. New Phytol. 155, pp 349–361.

Sun, L., Neville, R. A., Staenz, K., and White, H. P. (2008). Automatic destriping of Hyperion imagery based on spectral moment matching. Can. J. Remote Sens. 34(1), pp 68-81.

Swain, P. H. and Davis, S. M. (1978). Remote sensing: the quantitative approach. New York, McGraw-Hill.

Tan, K., Li, E., Giandu, and Peijun Du. (2014). Hyperspectral Image Classification Using Band Selection and Morphological Profiles. IEEE journal of selected topics in applied earth observations and remote sensing. 7(1).

Thenkabail, P. S., Enclona, E. A., Ashton, M. S. and Van der Meer, B. (2004). Accuracy assessments of hyperspectral waveband performance for vegetation analysis applications. Remote Sensing of Environment. 91(3-4), pp 354-376.

Tsai F and Philpot W. (1998). Derivative analysis of hyperspectral data. Remote Sens Environ. 66, pp 41–51. doi: 10.1016/S0034-4257(98)00032-7.

Tsai, F. and Philpot, W. D. (2002). A Derivative – Aided Image Analysis System for Land- Cover Classification. IEEE Trans. on Geoscienc and Remote Sensing. 40(2), pp. 416- 425.

Tsai, F. and Chen, W. W. (2008). Striping noise detection and correction of remote sensing images. IEEE Trans. Geosci. Remote Sens. 46(12), pp 4122-4131.

Underwood, E., S. Ustin, D. DiPietro (2003). Mapping native plants using hyperspectral imagery. Remote Sensing of Environ. 86, pp. 150- 161.

Ungar, S., Pearlman, J., Mendenhall, J. And Reuter, D. (2003). Overview of the Earth Observing One (EO-1) mission. IEEE Transactions on Geoscience and Remote Sensing. 41, pp. 1149–1159.

Ustin, S.L., Smith, M.O., Jacquemoud, S., Verstraete, M., and Govaerts, Y. (1999). Geobotany: Vegetation Mapping for Earth Sciences. In Renz, Andrew N. (ed), Remote Sensing for the Earth Sciences: Manual of Remote Sensing (3rd ed.), Vol 3. New York: John Wiley & Sons, pp. 189-248.

Ustin, S.L., João, M. (2011). Spectral identification of native and non-native plant Species. Santos University of California, Davis, CA, U.S.A. https://pdfs.semanticscholar.org/e835/c119d6708acc05d4c1060ab6cfbc6f4d5e45.pdf.

Vaiphasa, C. (2006). Remote sensing techniques for mangrove mapping Wageningen: Wageningen University.

Vane, G., Goetz, A.F.H. and Wellman, J.B. (1984). Airborne imaging spectrometer: a new tool for earth remote sensing. IEEE Trans. Geosci. Remote Sens. 22(6), pp 546–549.

Vane, G. and Goetz, A.F.H. (1988). Terrestrial Imaging Spectroscopy. Remote Sensing of Environment. 24, pp. 1-29.

Vane, G., Duval, J.E., and Wellman, J.B. (1993). Imaging Spectroscopy of the Earth and Other Solar System Bodies. In Pieters, Carle M. and Englert, Peter A.J. (eds.), Remote Geochemical Analysis: Elemental and Mineralogical Composition. Cambridge, UK: Cambridge University Press, pp. 121-143.

Vaughan, R.G., Calvin, W.M., Taranik, J.V. (2003). SEBASS hyperspectral thermal infrared data: surface emissivity measurement and mineral mapping, Remote sensing of environment. 85, pp 48-63.

Vermote, E. F., Tanre´, D., Deuze, J. L., Herman, M., and Morcrette, J. J. (1997). Second simulation of the satellite Data Sets, in the solar spectrum, 6S: an overview. IEEE Trans. Geosci. Remote Sens. 35, pp 675–686.

Wang, J. and Chang, C.I. (2006). Independent component analysis-based dimensionality reduction with applications in hyperspectral image analysis. IEEE Trans. Geosci. Remote Sens. 44, pp 1586–1600.

Wang, Y., Siemann, E., Wheeler, G.S., Zhu, L., Gu, X., Ding, J. (2012). Genetic variation in anti-herbivore chemical defences in an invasive plant. Journal of Ecology. 100, pp 894–904.

Webb A.R. (2002). Statistical Pattern Recognition (2nd ed.). New York: Wiley-Blackwell ltd., pp. 1-367.

Woolley, J. T. (1971). Reflectance and transmittance of light by leaves. Plant Physiology. 47, pp 656–662.

Wu, Y.Z., Chen, J., Ji, J.F., Tian, Q.J., & Wu, X.M. (2005). Feasibility of reflectance spectroscopy for the assessment of soil mercury contamination. Environmental Science & Technology. 39, pp 873-878.

www. photonics.com

www.geopool.fi

www.map.sedu.edu

Yang, C., Everitt, J.H., Davis, M.R. (2003). A CCD Camera-based Hyperspectral Imaging System for Stationary and Airborne Applications. Geocarto International.18(2).

Yang, C., Everitt, J.H., and Murden, D. (2010). Comparison of hyperspectral imagery with aerial photography and multispectral imagery for mapping broom snakeweed. International Journal of Remote Sensing. 31 (20), pp. 5423-5438.

Yokoya, N., Iwasaki, A. (2010). Preprocessing of hyperspectral imagery with consideration of smile and keystone properties. Article in Proceedings of SPIE - The International Society for Optical Engineering. DOI: 10.1117/12.870437.

Young, A, Britton, G. (1990). Carotenoids and stress. In Stress Responses in Plants: Adaptation and Acclimation Mechanisms; Alscher, R.G., Cummings, J.R., Eds.; Wiley: New York, NY, USA, pp. 87–112.

Zarco-Tejada, P. J., Miller, J. R., Noland, T. L., Mohammed, G. H., & Sampson, P. H. (2001). Scaling-up and model inversion methods with narrow-band optical indices for chlorophyll content estimation in closed forest canopies with hyperspectral data. IEEE Trans. Geosci. Remote Sens. 39(7), pp 1491 – 1507.

Zarco-Tejada, P.J., Pushnik, J.C., Dobrowski, S., Ustin, S.L. (2003). Steady-state chlorophyll a fluorescence detection from canopy derivative reflectance and double-peak red-edge effects. Remote Sensing of Environment. 84, pp 283–294.

Zhang, X., Friedl, M. A., Schaaf, C. B., Strahler, A. H., Hodges, J. C. F., Gao, F., Reed, B. C. and Huete, A. (2003). Monitoring vegetation phenology using MODIS. Remote Sensing of Environment. 84(3), pp 471-475.

Zhang, J., Rivard, B., Sánchez-Azofeifa, A., Castro-Esau, K. (2006). Intra- and interclass spectral variability of tropical tree species at La Selva, Rica: implications for species identification using HYDICE imagery. Remote Sensing of Environment. 105, pp 129–141.